
***The Framework Programme for Research & Innovation***
***Innovation actions (IA)***

*Project Title:*

**Autonomous self powered miniaturized intelligent sensor for environmental sensing and asset tracking in smart IoT environments**

# AMANDA

**Grant Agreement No: 825464**

**[H2020-ICT-2018-2020] Autonomous self powered miniaturized intelligent sensor for environmental sensing and asset tracking in smart IoT environments**

**Deliverable**

# D3.6 Power generation boards with appropriate measurement points and chosen MCU

| | | | |
|---|---|---|---|
| Deliverable No. | | **D3.6** | |
| Work package No. | **WP3** | Work package Title and task type | **Energy Autonomy Booster** |
| Task No. | **T3.4** | Task Title | **Power electronics interfacing with the main system microcontroller** |
| Lead beneficiary | | **CERTH** | |
| Dissemination level | | **PU** | |
| Nature of Deliverable | | **R** | |
| Delivery date | | **31 December 2021** | |
| Status | | **Final** | |
| File Name: | | **AMANDA_D3.6_Power_generation_boards_with_appropriate_measurement_points_and_chosen_MCU-v1.0** | |
| Project start date, duration | | **02 January 2019, 42 Months** | |

This project has received funding from the European Union's Horizon 2020 Research and innovation programme under Grant Agreement n°825464

## Authors List

| Leading Author | | | | |
|---|---|---|---|---|
| **Surname** | | **Initials** | **Beneficiary Name** | **Contact email** |
| Gkekas | | PG | CERTH | pangks@iti.gr |
| **Co-authors** | | | | |
| **#** | **Surname** | **Initials** | **Beneficiary Name** | **Contact email** |
| 1 | Kanlis | AK | CERTH | alexkanlis@iti.gr |
| 2 | Kouzinopoulos | CS | CERTH | kouzinopoulos@iti.gr |
| 3 | Sideridis | PS | CERTH | sideridis@iti.gr |
| 4 | Verikios | PV | CERTH | panos_verikios@iti.gr |

## Reviewers List

| List of Reviewers | | | | |
|---|---|---|---|---|
| **#** | **Surname** | **Initials** | **Beneficiary Name** | **Contact email** |
| 1 | De Vos | JD | EPEAS | julien.devos@e-peas.com |
| 2 | Stajic | SS | ZHAW | stji@zhaw.ch |

| Document history | | | |
|---|---|---|---|
| **Version** | **Date** | **Status** | **Modifications made by** |
| V0.1 | 16/03/2020 | Table of contents | CERTH |
| V0.2 | 22/04/2020 | Initial measurements with the off-the-shelf board | CERTH |
| V0.4 | 28/10/2020 | First iteration of the power electronics prototype | CERTH |
| V0.6 | 21/06/2021 | Second iteration of the prototype | CERTH |
| V0.8 | 22/11/2021 | Additional evaluation on the second iteration of the prototype | CERTH |
| V0.9 | 15/12/2021 | Submitted for internal review | CERTH |
| V1.0 | 28/12/2021 | Final version, ready for submission | CERTH, ZHAW, EPEAS |

## List of definitions & abbreviations

| Abbreviation | Definition |
|---|---|
| ASSC | Autonomous Smart Sensing Card |
| BLE | Bluetooth Low Energy |
| BOM | Bill of Materials |
| CSP | Chip Scale Package |
| EH | Energy Harvester |
| IC | Integrated Circuit |
| LDO | Low-Dropout regulator |
| MCU | Microcontroller Unit |
| MOSFET | Metal Oxide Semiconductor Field Effect Transistor |
| MPPT | Maximum Power Point Tracking |
| OCV | Open Circuit Voltage |
| PLL | Phase-Locked Loop |
| PMIC | Power Management Integrated Circuit |
| PV | Photovoltaic |
| QFN | Quad Flat No-lead |
| RTC | Real Time Clock |
| SMPS | Switched-mode Power Supply |

## Executive Summary

Deliverable D3.6 details the work performed as part of Task T3.4. **Task T3.4 - Power electronics interfacing with the main system microcontroller** is part of **WP3 - Energy Autonomy Booster** of the AMANDA project. The aim of WP3 is to develop a power module that includes energy generation, regulation and storage. Task T3.4 focuses on the integration of the energy-providing components, the hardware management for that energy and the storage element. Part of the energy management is performed in hardware, while another part is done in firmware. The MCU is also an integral part of the power module, as it distributes energy to various parts of the system and subsequently ensures that it is used properly. The Task is further divided into the following subtasks:

- Creating a block diagram for the power electronics prototype that includes the power management, energy storage and MCU of the system, together with all elements required to monitor the system and shut down certain parts
- Performing a simulation of the resulting circuit to investigate the efficiency of the elements, leakages and the energy intake under specific illumination conditions
- Draw and review the schematics of the above circuit as well as generate and review the corresponding PCB layout
- Fabricate the PCBs of the power electronics prototype through an external manufacturer, populate them and perform basic testing
- Optional redesign of the system for optimisation

This Deliverable was used as an input for the development of the size-unconstrained prototype of **T5.1 - First size unconstrained design and prototype.** It will also be used for the development of the miniaturised prototype, as an input for **Deliverable D5.2 - Miniaturized PCB Prototype.** Moreover, it will be utilised for the evaluation of both the individual components and the final, integrated system, as part of **Deliverables D6.2 - Characterisation/test reports of individual components in lab environment** and **D6.3 - Characterisation/test reports of integrated AMANDA platform in lab environment** respectively.

# Table of Contents

## List of Figures



## List of Tables

# 1 Introduction

The purpose of **Deliverable D3.6 - Power generation boards with appropriate measurement points and chosen MCU** is to present the effort, spent as part of **Task T3.4 - Power electronics interfacing with the main system microcontroller**, towards the development of a power electronics prototype. The prototype includes the power electronics of the card, the circuits that are used to produce electrical energy, control its flow on the card and store it. Their function is generally to process and control the electrical energy, by supplying voltage and current in a form that is optimally suited to the load [1]. Figure 1 presents a general flowchart of electric power conversion.

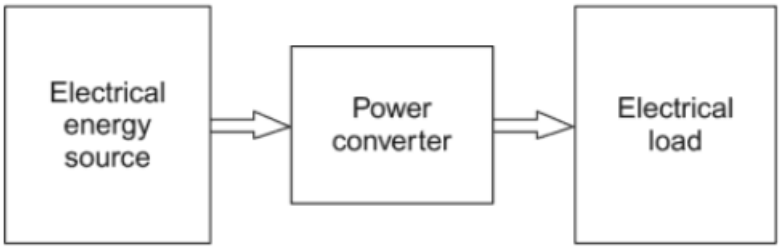


Figure 1 General system for electric power conversion [2]

A conceptual architecture of the AMANDA card is detailed in **Deliverable D1.12 - Architecture design of the AMANDA system delivered (for both breadboard and integrated/miniaturised system) v3,** as presented in Figure 2**.** The ASSC includes:

- The **Sensor and Edge Intelligence** block, which incorporates the sensing and processing capabilities of the ASSC
- The **Wireless and Security** block that includes the communication tools as well as the software and hardware security mechanisms of the card
- The **Energy Management** block that involves the power electronics of the ASSC

The Energy Management block includes the power electronics components of the AMANDA ASSC:

- PV cells for energy harvesting
- PMIC for energy management
- Energy storage device for storage of surplus energy

The MCU, albeit not a power electronics component, is an important part of the energy management block of the ASSC. It is responsible for the management and distribution of the energy produced by the energy harvester or stored in the energy storage to different components of the system and ensures that that energy is utilised in an efficient way and not wasted by parts that are not active. The development of the energy management block was therefore based on the interfacing between the power electronics and the MCU.

The efficiency of the power processing elements, in terms of energy conversion, consumption and leakages is crucial, especially in a low-power environment such as the AMANDA card. The aim of T3.4 is to bring together the components of the energy management block of AMANDA, together with the MCU. For these components, their efficiency in terms of energy consumption is evaluated; their leakages are measured while the energy intake of the PV under specific illumination conditions is provided.

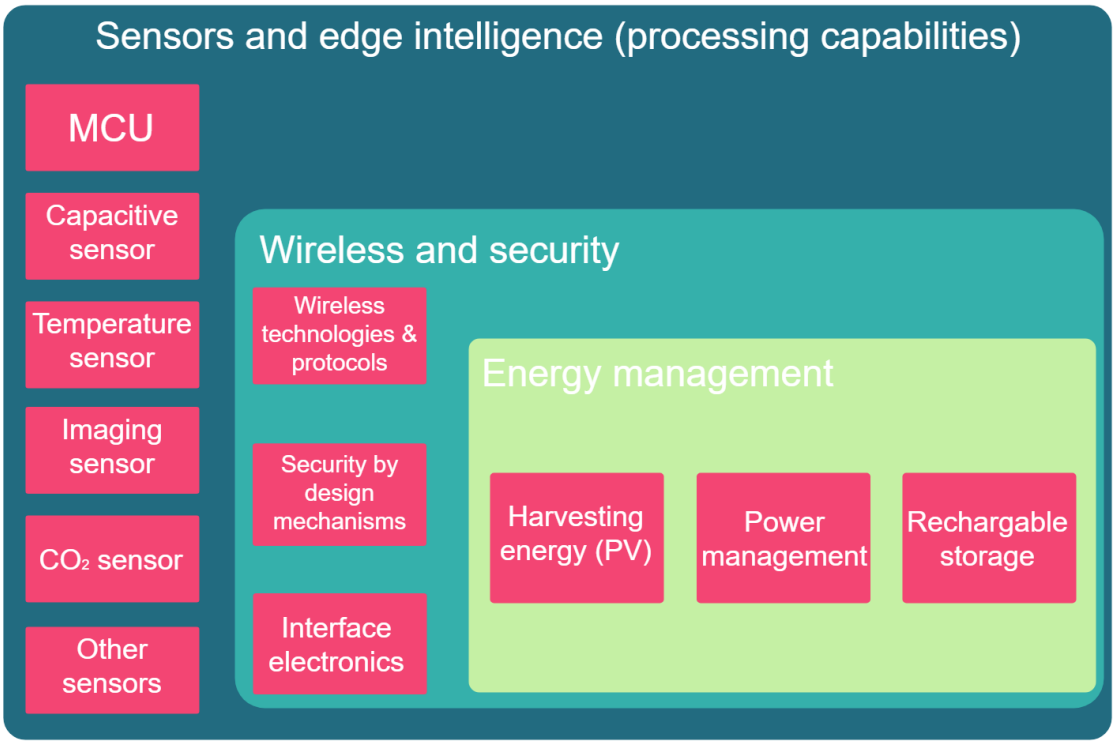


Figure 2 Conceptual architecture of the AMANDA ASSC

To validate the architecture of the system, as it has been defined in the early stages of the project, and to optimise it in terms of functionality, power consumption and size, a power electronics prototype was developed that includes the power electronics and the MCU of the ASSC. The power electronics prototype was based on the size-unconstrained prototype of AMANDA. For the development of the prototype, an iterative process was followed, as part of the *system integration and prototyping phase* of the project. The iterative integration process is depicted in Figure 3 below.

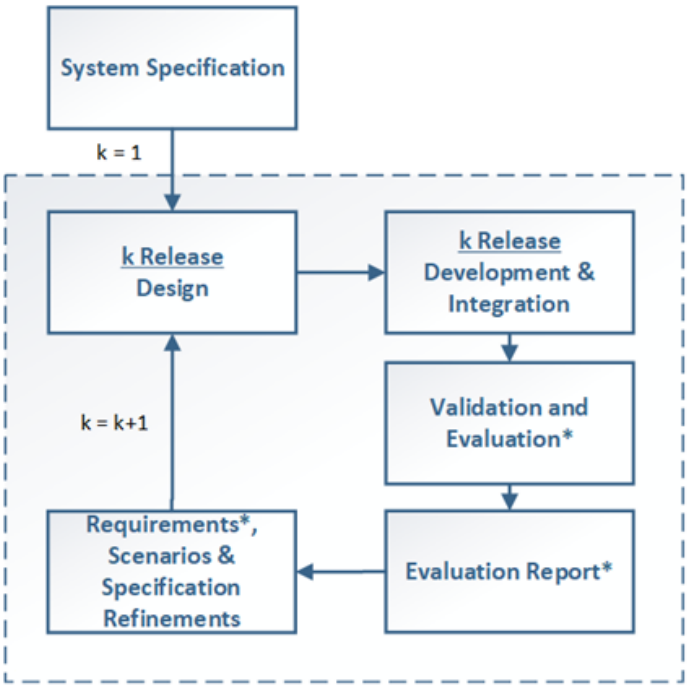


Figure 3 Iterative integration process

The main consideration behind the prototype's development was its optimisation in terms of energy efficiency; the prototype was also evolved through different iterations to enable the easier and more accurate evaluation of the individual components and the interaction between the MCUs and power electronics. The output of T3.4 was used throughout the duration of **T5.1 - First size unconstrained design and prototype** for the development and optimisation of the size-unconstrained prototype of the AMANDA ASSC and will also be used as an input for **T5.2 - Miniaturized PCB design and prototype development**.
This Deliverable is structured as follows:

- Section 1 provides an introduction to the process followed for the design and development of the power electronics prototype
- Section 2 details the functional description as well as full technical specifications and the main functionality of the system's power electronics, together with the technical specifications of the system's MCU. Moreover, the architecture of the prototype is introduced
- Section 3 presents the development process of the different iterations of the porotype, including technical specifications and details about the PCB manufacturing process
- Section 4 provides an evaluation of the different iterations of the power electronics prototype
- The BOM of the prototype is given in the Appendix of this document

# 2 Prototype components and architecture

This Section details the different components and the architecture of the power electronics prototype. It is organised as follows:

- Section 2.1 details the energy management block and provides the specifications of its components
- Section 2.2 lists the specifications of the MCU
- Section 2.3 discusses the architecture of the power electronics prototype

## 2.1 Energy management block

The purpose of the power electronics is to supply the different components of the AMANDA ASSC with continuous power. The energy management block consists of a PV energy harvester, a PMIC as well as a rechargeable storage element. Figure 4 depicts the components of the energy management block.

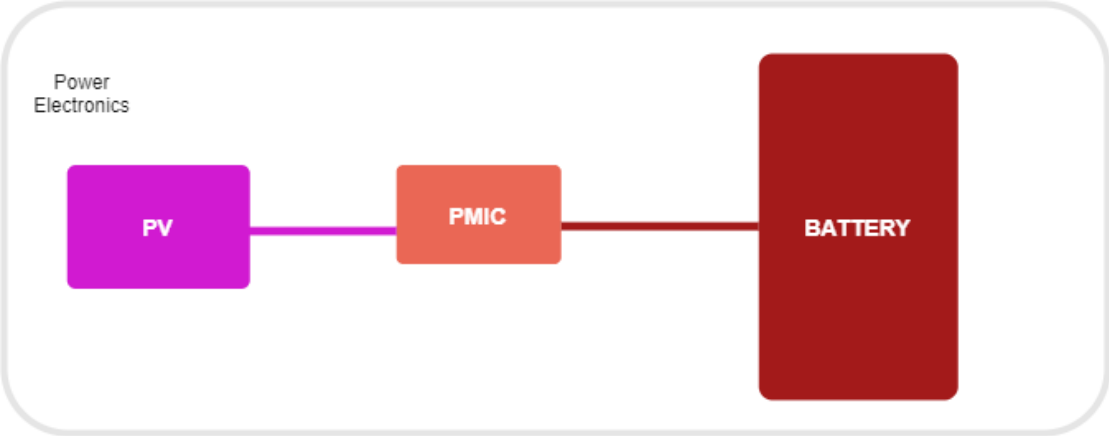


Figure 4 Components of the energy management block

Table 1 below presents an overview of the components of the energy block, including a description of each component as well as its manufacturer.

| Power electronics | | |
|---|---|---|
| **Name** | **Description** | **Manufacturer** |
| Rechargeable energy storage | 2mAh, 3-4V, battery | ILIKA |
| PV cell | ExCellLight EXL-1V50-SM / ExCellLight EXL-1V20-SM | Lightricity |
| PMIC | AEM10941 - solar energy harvesting IC solution | EPEAS |

Table 1 Power electronics overview

### 2.1.1 Energy harvester

The PV energy harvester has been developed by Lightricity and is tasked with the conversion of ambient light, both indoor and outdoor, into electrical energy. The harvested energy is then delivered to the system's circuitry through the PMIC. The different specification, design and development phases of the energy harvester were presented in detail in the following Deliverables:

- **D3.1 - PV Energy Harvester Specifications.** Includes detailed specifications for the PV energy harvester technology, including a definition of the process flow for the PV and

the specification of the component's features, including its performance and footprint. Moreover, it includes details on the fabrication and characterisation of the PV cells

- **D3.2 - PV Energy Harvester Fabrication and Testing.** Includes details on the fabrication and validation of the PV cells
- **D3.3 - PV Energy Harvester Proof-of-concept prototype.** Reports on the optimised process flow of the PV cells for cost reduction

The EH component should provide more power than the average energy consumption of the MCU of the prototype board. The amount of power provided by the energy harvester depends mainly on the illumination levels, that are generally influenced by the location of the PV cells; the luminosity indoors is often much lower than the outdoors' luminosity. Therefore, the EH component should provide an average power of at least 10μW, which corresponds to the consumption of the basic MCU low-power mode.
Table 2 below provides an indicative list of typical lux levels found both in indoors and outdoors environments, together with the power generated by the Lightricity PV.

| **Environment** | **Typical lux** | **Estimated PV power density** |
|---|---|---|
| Dim corridor/underground parking | 50 - 100 lux | 0.005 - 0.01mW / $cm^2$ |
| Restroom | 100 - 300 lux | 0.01 - 0.03mW / $cm^2$ |
| Homes | 200 - 400 lux | 0.02 - 0.04mW / $cm^2$ |
| Office - Open | 300 - 500 lux | 0.03 - 0.05mW / $cm^2$ |
| Kitchen | 300 - 750 lux | 0.03 - 0.075mW / $cm^2$ |
| Hypermarket/warehouse | 1000 lux | 0.1mW / $cm^2$ |
| Outside under shading or clouds | 3000 - 10000 lux | 0.3 - 1mW / $cm^2$ |
| Bright sunlight | > 100000 lux | > 10mW / $cm^2$ |

Table 2 Typical indoor and outdoor illumination levels

As discussed in **Deliverable D3.3 - PV Energy Harvester Proof-of-concept prototype**, Lightricity's indoor energy harvester will need to compete with the current and emerging technologies targeting indoor applications. Other emerging technologies such as dye-sensitized or organic photovoltaics may exhibit slightly higher performance than Silicon, but suffer indoors from stability issues that are unlikely to be solved in the short-to-medium term. Lightricity's performance of their larger scale energy harvesting prototypes is a key enabling technology, providing the power requirements of the ASSC and the power electronics prototype.
Table 3 and Table 4 below list the performance characteristics of the EXL-1V50-SM and EXL-1V20-SM modules respectively for a 200 lux white LED spectrum. Figure 5 and Figure 6 depict the current-voltage curves of the modules for different illumination levels; 94, 200, 500 and 1000 lux. Finally, Table 5 presents the mechanical characteristics of the developed PV energy harvester.

| **Target performance** | **Module EXL-1V50-SM** |
|---|---|
| | **200 lux white LED spectrum** |
| Size / Thickness | 23.8 x 10.2mm / <1mm |
| Active area | 2.15$cm^2$ |
| Number of cell(s) | 1 |
| Open circuit voltage | 1.15V |
| Short circuit current | 49.8μA |

| | |
|---|---|
| Operating voltage | 1.0V |
| Operating current | 47.6µA |
| Operating power | 47.6µW |
| Power density (active area) | >20µW/cm$^2$ |
| Cell efficiency | >30% |

Table 3 ExCellLight EXL-1V50-SM performance and functionality

| **Target performance** | **Module EXL-1V20-SM** |
|---|---|
| | **200 lux white LED spectrum** |
| Size / Thickness | 11.65 x 8.85mm / <1mm |
| Active area | 0.98cm$^2$ |
| Number of cell(s) | 1 |
| Open circuit voltage | 1.15V |
| Short circuit current | 22.7µA |
| Operating voltage | 1.0V |
| Operating current | 21.7µA |
| Operating power | 21.7µW |
| Power density (active area) | >20µW/cm$^2$ |
| Cell efficiency | > 30% |

Table 4 ExCellLight EXL-1V20-SM performance and functionality

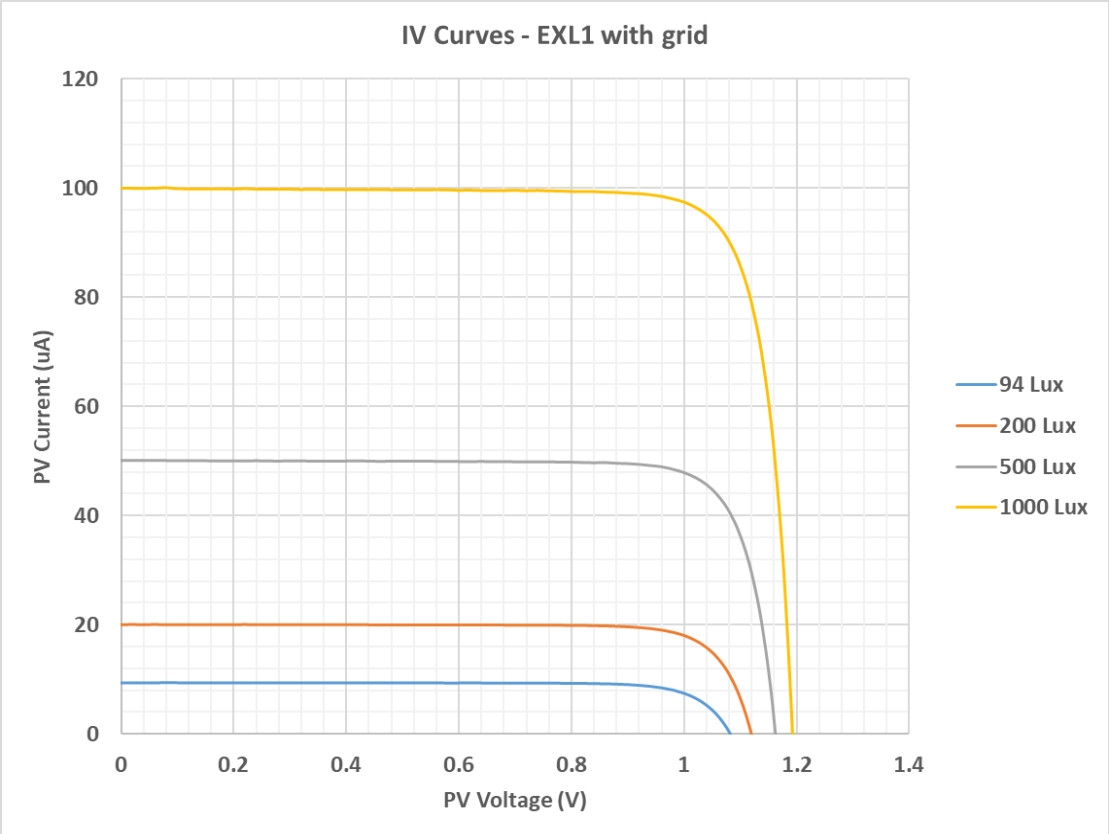


Figure 5 Current-Voltage curves for various illumination levels (EXL-1V20-SM/EXL1)

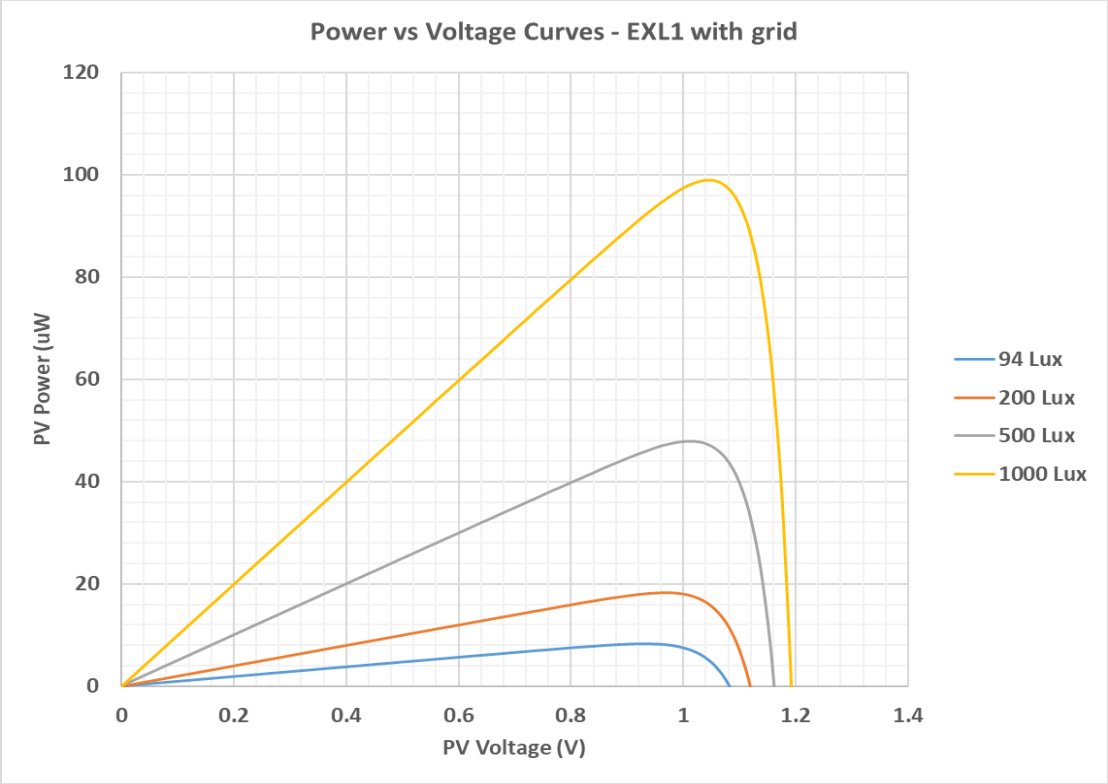


Figure 6 Power-Voltage curves for various illumination levels (EXL-1V20-SM/EXL1)

| Geometrical parameters | Target |
|---|---|
| Shape | Rectangular |
| Outer module dimensions | 2.4 x 1.0cm or less |
| Thickness | < 1mm |
| Connection method | SMT |

Table 5 Mechanical information on the PV harvester

### 2.1.2 PMIC

The PMIC of the ASSC has been developed by EPEAS, as described in **Deliverable D3.4 - Report on Power management electronics.** It is responsible for the distribution of energy between the different components of the system, including the sensors, the microcontroller and the wireless communication circuits as well as for the provision of the system with different regulated voltages. The PMIC harvests solar energy through the energy harvester from Lightricity described in Section 2.1.1 above, stores that energy to the rechargeable storage element from ILIKA described in Section 2.1.3 below and supplies the system with the desired regulated voltages. As described in D3.4, the PMIC has two regulated outputs that are used to supply the application circuitry. A first output AOOUT deliver a 2.2V voltage to the always-on peripherals that are required to wake up the system while LVOUT supplies the microcontroller.

The PMIC was first planned to have a third output to supply the high-voltage loads, but for a number of reasons detailed in D3.4 it was decided to use instead an external DC-DC converter connected directly to the storage device. This converter can be enabled or disabled by the PMIC.

Due to the COVID 19 pandemic and supply-chain major issues in the semiconductor market, the prototyping of the PMIC was delayed. It has now been manufactured and its validation

will start early 2022. Meanwhile EPEAS proposed to replace the dedicated PMIC by AEM10941 [3], which is commercially available.
The power electronics prototype uses the AEM10941 PMIC of EPEAS, depicted in Figure 7. The electrical specifications of the device are given in Table 6 below.

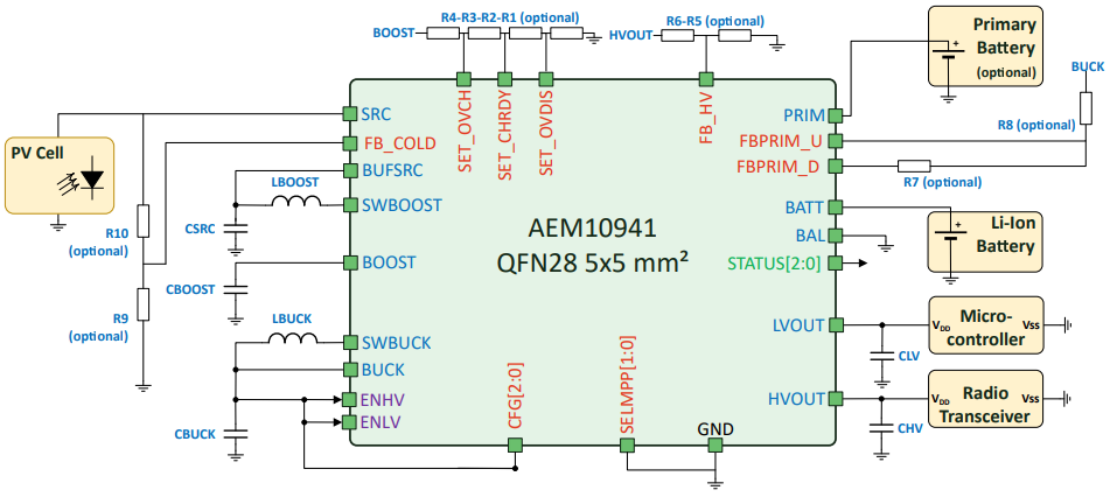


Figure 7 The AEM10941 PMIC

| Symbol | Parameter | Conditions | Min | Typ | Max | Unit |
|---|---|---|---|---|---|---|
| **Power Conversion** | | | | | | |
| $P_{SRC,CS}$ | Source power required for cold start (CS) | During CS | | 2 | | µW |
| $V_{SRC}$ | Input voltage of the energy source | During CS | 0.3 | | 5 | V |
| | | After CS | 0.05 | | 5 | V |
| $R_{MPPT}$ | MPPT ratio | | 65, 70, 75, 80, 85 or 90 | | | % |
| $V_{BOOST}$ | Output of the boost converter | Normal operation | 1 | | 4.5 | V |
| $V_{DDINT}$ | Internal supply | Normal operation | 1.98 | 2.2 | 2.42 | V |
| **Storage element** | | | | | | |
| $V_{BAT}$ | Voltage on the storage element. | Rechargeable battery | 1 | | 4.5V | V |
| $T_{CRIT}$ | Time before shutdown after STATUS[0] has been asserted | | 400 | 600 | 800 | ms |
| $V_{OVCH}$ | Maximum voltage accepted on the storage element before disabling the boost converter | | | 4 | | V |
| $V_{CHRDY}$ | Minimum voltage required on the | | | 3.4 | | V |

| | | | | | | |
|---|---|---|---|---|---|---|
| | storage element before enabling the power gating switch and the high-voltage buck-boost | | | | | |
| $V_{OVDIS}$ | Minimum voltage accepted on the storage element before entering into a shutdown | | | 3 | | V |
| **Load output voltage** | | | | | | |
| $I_{AOOUT}$ | Current drive capability on the AO-OUT output | | | | 10 | µA |
| $V_{AOOUT}$ | Always-On output voltage | | 1.98 | 2.2 | 2.42 | V |
| $I_{LVOUT}$ | Current drive capability on the LVOUT output | | | | 60 | mA |
| $V_{LVOUT}$ | LVOUT output voltage | | 1.98 | 2.2 | 2.42 | V |
| **Internal supply & quiescent current** | | | | | | |
| $V_{DDINT}$ | Internal voltage supply | | | 2.2 | | V |
| $I_{DDINT}$ | | | | 200 | | nA |
| **Logic output pins** | | | | | | |
| STA-TUS[0:1] | Logic output levels on the status pins | Logic high | | $V_{DDINT}$ | | V |
| | | Logic low | | 0 | | V |
| CFGOUT | Data output to acknowledge programming of the PMIC | Logic high | | $V_{DDINT}$ | | V |
| | | Logic low | | 0 | | V |

Table 6 AEM10941 specifications

AEM10941 harvests an input current of up to 110mA. It integrates an ultra-low-power boost converter to charge a storage element. The boost converter operates with 50mV to 5V input voltages. It can start its operation with uncharged storage elements at an input voltage of 380mV and an input power of 3µW. The low-voltage supply typically drives an MCU at 1.2V or 1.8V. The high-voltage supply typically drives a radio transceiver at a configurable voltage between 1.8V and 4.1V. Both are driven by highly-efficient LDO regulators.
The PMIC will be encapsulated into QFN 28 5 x 5 x 0.5mm pitch packages as shown in Figure 8 below. The exposed pad provides a strong connection to the ground plane.

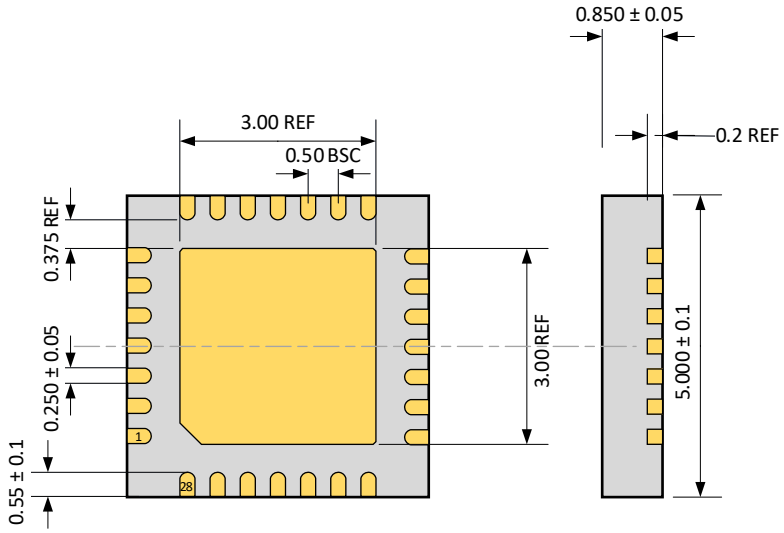


Figure 8 Footprint layout QFN28 - 5 x 5mm

### 2.1.3 Storage element

The energy storage element has been developed by ILIKA according to the requirements of the AMANDA ASSC. **Deliverable D3.5 - Report on Rechargeable Storage Element** presents detailed information on the development and characterisation of the energy storage component.

The purpose of the ILIKA thin-film battery is to provide an energy storage element that will allow the AMANDA ASSC to operate in cases where there is insufficient power from the energy harvesting component, such as in the presence of peaks in the power consumption of the ASSC. For the rechargeable energy storage element, seven higher-energy-density M300 cells are used per card. Each M300 cell is constructed from a stack of six different M50 cells, therefore a total of 42 cells are used. Figure 9 presents the overview of a micro-fabricated Stereax cell while Table 7 lists the specifications for the rechargeable storage element.

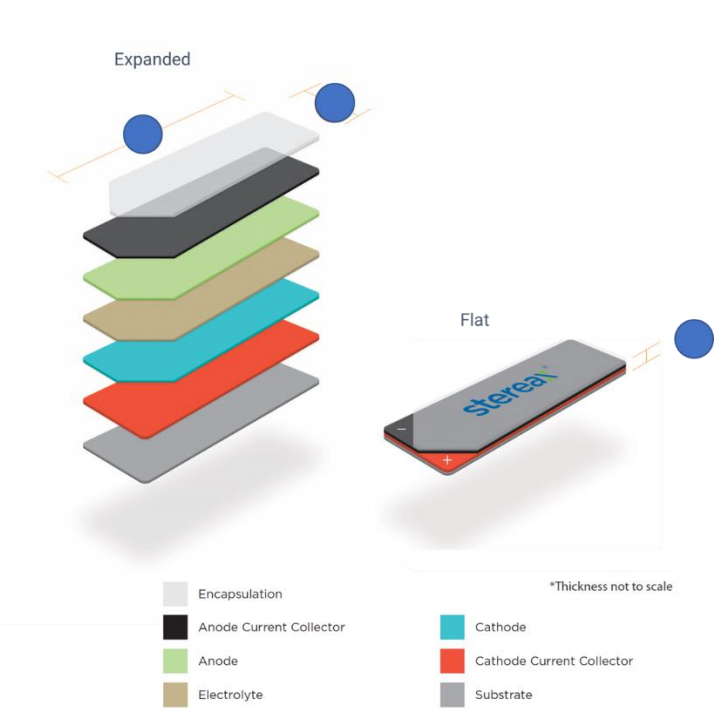


Figure 9 Schematic of a micro-fabricated Stereax cell

| Energy Storage | Target |
|---|---|
| Rated Capacity | 2mAh |
| Voltage | 3 - 4V |
| Standard continuous discharge current | 2mA |
| Peak current (< 0.5ms pulse) | 40mA |
| Active Footprint | 88% |
| Quiescent/leakage current | < 10nA |
| Continuous current | 20mA |
| Coulombic Efficiency | > 99.95% |
| Footprint (of all cells) | 24 x 14mm |

Table 7 The AMANDA rechargeable storage element specifications

The performance criteria of the M300 cells have yet to be fully quantified and this process is delayed due to the ongoing effects of the COVID-19 pandemic. Moreover and due to global supply chain issues, ILIKA will provide the completed M300 cells at a later stage of the project. In mitigation, ILIKA proposed to purchase commercially available thin cells from Powerstream to assist in the evaluation of the size-unconstrained and miniaturised prototypes of the card, until M300 is delivered.

Table 8 lists the technical specifications[1] of the Powerstream GEB201212C polymer Lithium-ion battery, while Table 9 details its performance characteristics.

| Characteristic | | Specifications | Remark |
|---|---|---|---|
| Nominal capacity | | 10mAh | 0.2$C_5$A discharge |
| Nominal voltage | | 3.7V | Average voltage at 0.2$C_5$A discharge |
| Charge current | | • Charge current standard: 0.2 $C_5$A<br>• Max: 1$C_5$A | Working temperature：0~45°C |
| Charge cut-off voltage | | 4.20 ± 0.05V | |
| Discharge current | | • Continuously: 10$C_5$A<br>• Max: 15$C_5$A | Working temperature：0~60°C |
| Discharge cut-off voltage | | 2.75V | |
| Cell voltage | | 3.8 ~ 4.0V | When leave factory |
| Impedance | | ≤ 650mΩ charge | AC 1KHz after 50% charge |
| Weight | | Approximately 0.5g | |
| Storage temperature | ≤ 1 month | -20 ~ 45°C | Best 20 ± 5°C for long-time storage |
| | ≤ 3 months | 0 ~ 30°C | |
| | ≤ 6 months | 20 ± 5°C | |
| Storage humidity | | 65 ± 20% RH | |

[1] *An important characteristic of a battery is $C_i$ - The rated capacity, in ampere-hours, for a specific, constant discharge current (where i is the number of hours the cell can deliver this current). For example, the $C_5$ capacity is the ampere-hours that can be delivered by a cell at a constant current in 5 hours. As a cell's capacity is not the same at all rates, $C_5$ is usually less than $C_{20}$ for the same cell.*

Table 8 Technical specifications of Powerstream GEB201212C [1]

| Item | Test Methods | Performance |
|---|---|---|
| 0.2C capacity | After standard charging, laying the battery for 0.5h, then discharging at $0.2C_5A$ to voltage 2.75V, recording the discharging time | ≥ 300 minutes |
| 8C discharge | After standard charging, laying the battery for 0.5h, then discharging at $8C_5A$ to voltage 2.75V, recording the discharging time | ≥ 6.5 minutes |
| Cycle life | Constant current $1C_5A$ charge to 4.2V, then constant voltage charge to current declines to 0.05C5A, stay 5min, constant current $1C_5A$ discharge to 2.75V, stay 5min. Repeat above steps till continuously discharging time less than 36 minutes | ≥ 300 times |
| Capability of keeping electricity | 20 ± 5°C, After standard charging, laying the battery 28days, discharging at 0.2C5A to voltage 2.75V, recording the discharging time | ≥ 240 minutes |
| Shelf life | After standard full charging, laying the battery in a storage room at 20 ± 5°C, until the OCV reaches 3.4V, recording the days | Approximately 365 days |

Table 9 Performance characteristics of the Powerstream GEB201212C [1]

## 2.2 Microcontroller Unit

For the MCU of the ASSC, the STM32L496 ultra-low power microcontroller from ST Microelectronics was chosen. The processor is based on the high performance ARM Cortex-M4 32-bit RISC core with a floating-point unit single-precision that supports all ARM single-precision data-processing instructions and data types. Furthermore, it implements a full set of DSP instructions as well as a memory protection unit, which enhances application security. An external SMPS, an electronic power supply that includes a switching regulator in order to convert electrical power in an efficient manner and transfer power to DC loads, is used instead of an integrated LDO in order to optimise power consumption. Figure 10 depicts the MCU of the prototype including SMPS.


Figure 10 The MCU including SMPS

The technical specifications of the MCU such as the performance features, the available peripherals and interfaces are presented in detail in **Deliverable D1.11 - Full System specification & BOM v3**. This Section provides information on the electrical characteristics of the MCU as well as the available power modes that the microcontroller supports. In order to analyse the power consumption of the MCU, all its characteristics that affect the consumption such as the system clock sources and the different low-power modes are also presented.

### 2.2.1 Technical specifications

Table 10 below lists the electrical characteristics of the STM32L496 MCU.

| Symbol | Parameter | Min | Typ | Max | Unit |
|---|---|---|---|---|---|
| VDD | Supply voltage | 1.71 | | 3.6 | V |
| VDDA | Supply voltage for analog parts | 1.62 | | 3.6 | V |
| VDDUSB | External supply for USB transceivers | 3 | | 3.6 | V |
| VDD12 | SMPS supply voltage | 1.05 | | 1.32 | V |
| VDDIO2 | External power supply for 14 I/Os | 1.08 | | 3.6 | V |
| VLCD | Supply for the LCD controller | 2.5 | | 3.6 | V |
| VBAT | Supply for internal RTC and backup registers | 1.55 | | 3.6 | V |
| Fclk | Clock frequency | | | 80 | MHz |
| T | Operating temperature | -40 | | 125 | °C |

Table 10 Electrical characteristics of the MCU

The MCU has the ability to run with a clock frequency of up to 80MHz, with four different clock sources available that can be used to drive the system clock according to the desired functionality and consumption. The clock sources of the MCU are the following:

- A high-speed external crystal or ceramic resonator (HSE) with a frequency range of 4-48MHz, which can supply a PLL. This crystal can also be configured in bypass mode for an external clock
- A high-speed internal RC oscillator at 16MHz (HSI16), that is trimmable by software and can be used to supply the PLL of the system
- A multi-speed internal RC oscillator (MSI), which is also trimmable by software and has the ability to generate 12 frequencies from 100kHz to 48MHz. The MSI can supply a PLL. When a 32.768kHz clock source is available in the system as a Low Speed External oscillator (LSE), the MSI frequency can be automatically trimmed by hardware to reach better than ±0.25% accuracy
- A system PLL, which can be fed by all the clock sources above, with a maximum frequency of 80MHz

Apart from the Run mode, which is the default state after a system or a power reset, the MCU supports seven low-power modes in order to achieve the best compromise between low-power consumption, short start -up time, available peripherals and available wakeup sources. The low-power modes that are supported by the MCU are presented in Table 11 below, as detailed in [4].

| Low-power mode | Description |
|---|---|
| **Sleep mode** | In this mode the CPU is stopped, while all peripherals continue to operate. The peripherals can wake up the CPU when an interrupt event occurs |
| **Low-power run mode** | The low-power regulator is used for the supply of the core in this mode in order to minimize the current consumption of the regulator. The clock frequency of the core is limited to 2MHz while the peripherals can be driven by HSI16. Both SRAM and Flash memory can be used for code execution |
| **Stop 0, 1, 2** | The available Stop modes can be used in order to achieve the lowest power consumption while retaining the content of SRAM and registers. This is accomplished because the clock sources for the CPU are stopped and all the rest of the clock sources of the system are disabled apart from the low speed internal oscillator. The system can wake up either with the use of the RTC, which can remain active, or with some available peripherals with wakeup capability. Three Stop modes are available:<br>• **Stop 0.** The main regulator remains ON, allowing a very fast wakeup time but with a much higher energy consumption<br>• **Stop 1.** It offers the largest number of active peripherals and wakeup sources, a smaller wakeup time but a higher energy consumption than Stop 2<br>• **Stop 2.** In Stop 2 mode, most of the VCORE domain is in a lower leakage mode<br>When exiting from Stop 0, Stop 1 or Stop 2 modes, the system clock can be either MSI up to 48 MHz or HSI16, depending on software configuration |
| **Standby** | This mode is used to achieve the lowest power consumption with the core of the system completely powered down. All the available clock sources are also switched off. The RTC and the brown-out reset can remain active. The state of each I/O during standby mode can be selected by software. Only the registers in the backup domain and standby circuitry are retained when this mode is entered. The low-power regulator can be used in order to retain the contents of the SRAM2 memory. The system exits standby mode when a wake up detects an event. An exit from the standby mode can be also triggered with the use of the RTC or on external reset events. In these cases, the microcontroller can run up to 8MHz using the MSI clock source |
| **Shutdown** | The Shutdown mode can achieve the lowest power consumption. The internal regulator is switched off so that the |

| | |
|---|---|
| | VCORE domain is powered off. The PLL, the HSI16, the MSI, the LSI and the HSE oscillators are also switched off. The RTC can remain active. The brown-out reset is not available in this mode. No power voltage monitoring is possible in this mode, therefore the switch to Backup domain is not supported. All the memory and register contents are lost except for registers in the Backup domain. The device exits Shutdown mode when an external reset, a wake up pin event, or an RTC event occurs. After exiting this modes the microcontroller clock can run up to 4MHz |

Table 11 Low-power modes of MCU

STM32L496 integrates two linear voltage regulators that supply most of the digital parts of the microcontroller. The main regulator and the low-power regulator. The main regulator is used in the Run and Sleep modes and in the Stop 0 mode. The low-power regulator is used in Low-Power Run, Low-Power Sleep and in Stop 1 and 2 modes. Moreover, it is can be used to supply the SRAM2 in Standby mode with SRAM2 retention as mentioned in Table 11. Both of the embedded regulators are completely powered down in standby and shutdown mode resulting in the lowest power consumption since the CPU is switched off. Furthermore, the MCU supports dynamic voltage scaling to optimize its power consumption in run mode. Dynamic voltage scaling helps to balance power consumption with processing demand. The voltage from the main regulator that supplies the logic core can be adjusted according to the system's maximum operating frequency. There two supported ranges are presented in Table 12.

| **Range** | **CPU frequency** |
|---|---|
| Range 1 | Up to 80MHz |
| Range 2 | Up to 26MHz |

Table 12 Power consumption ranges

When the core voltage is supplied by the low-power regulator and the main regulator is switched off, the system enters a low-power run mode. As mentioned in Table 11, the CPU can run up to 2MHz in this mode, while the peripherals with independent clock can be driven by the high-speed internal oscillator. When the main regulator is in use, the STM32L496 package with the external SMPS option permits to force an external supply voltage for the core on the VDD12 supply pins. When VDD12 is forced by an external source and is higher than the output of the internal LDO, the current is taken from this external supply and the overall power efficiency is significantly improved if using an external step down DC-DC converter. The external SMPS version of SMT32L496 is used for the AMANDA system in order to maximise further the lifetime of the battery of the ASSC. The DC-DC converter generates a VCORE logic supply instead of using the integrated LDO extending that way the power efficiency in Run modes. The SMPS is connected to the VDD12 pin of the MCU. The expected power consumption gain in Run modes can be up to approximately 60% depending on the supply voltage.

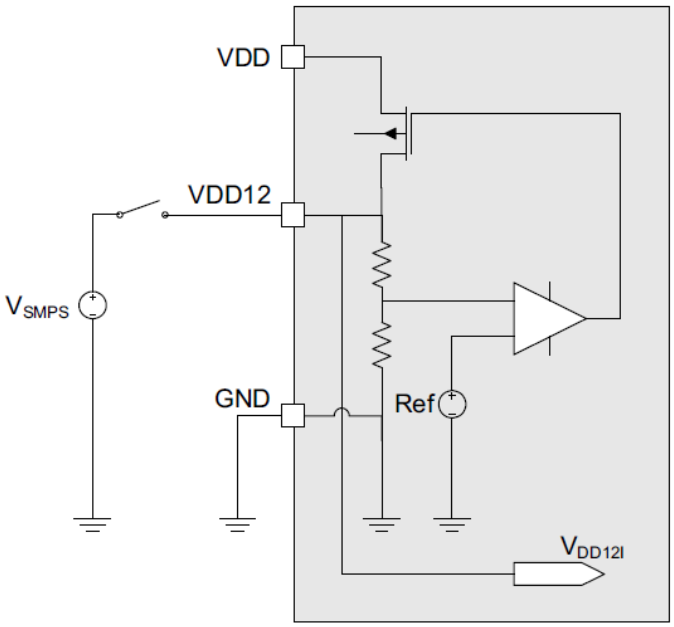


Figure 11 SMPS

According to [5], in case the external power supply connected to the VDD12 pin exceeds the internally generated voltage of VDD12I, the main regulator is automatically disabled and the digital current is provided by the external source as depicted in Figure 11. As VDD12 shares the same pin as the output of the internal regulator, applying a voltage that is at least 50mV higher than the VDD12I on the VDD12 blocks the PMOS and the regulator consumption is negligible.
The block diagrams presented in Figure 12 and Figure 13 illustrate the two supply options.

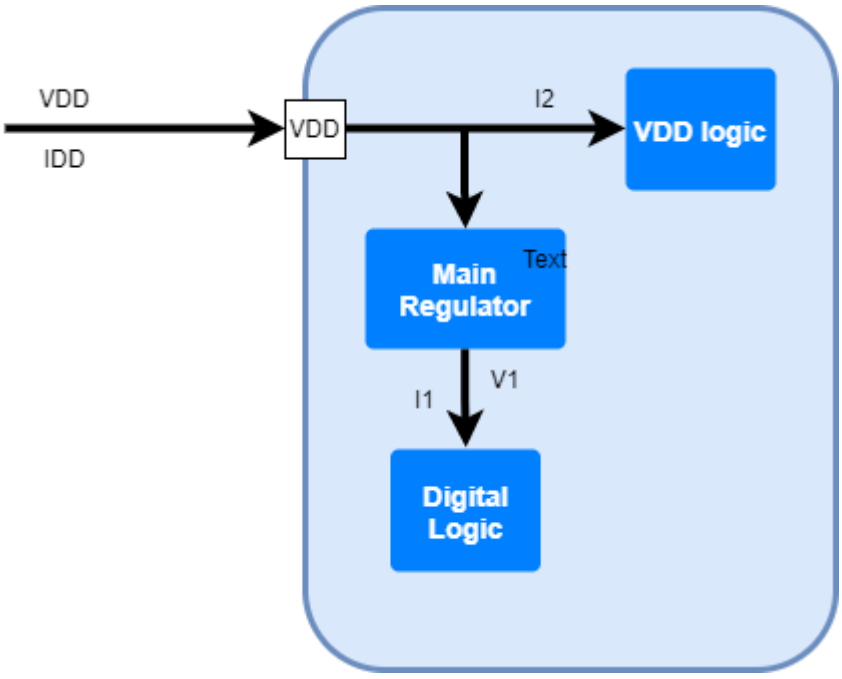


Figure 12 Supply without SMPS

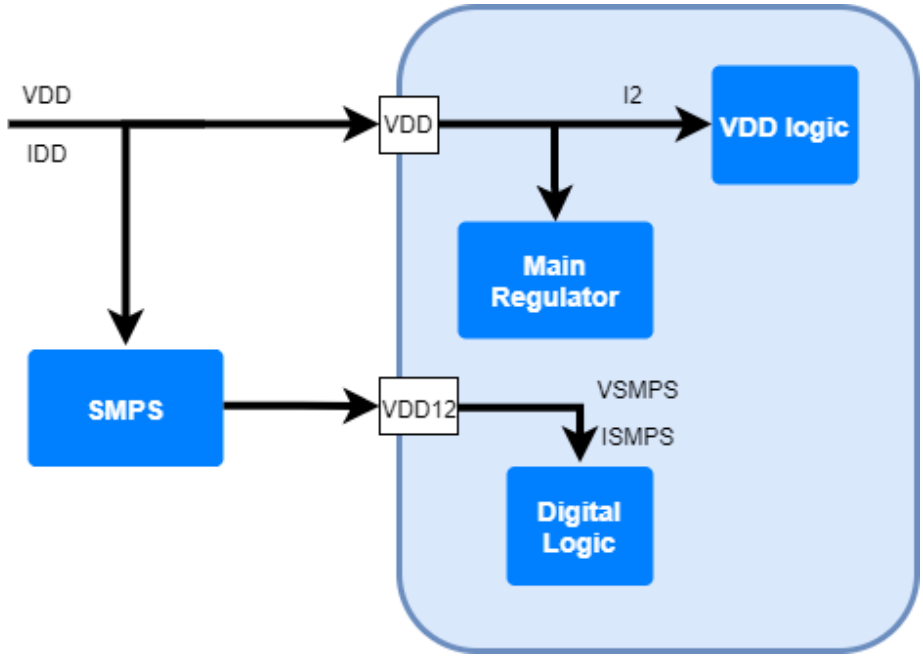


Figure 13 Supply with SMPS

When the digital core logic is supplied by the SMPS, the consumption becomes:

$$I_{SMPS} = I_1 * V_{SMPS}/V_1$$

due to the change of its supply source. If the efficiency of the SMPS is *n*, the overall consumption becomes:

$$I_{DD} = I_2 + I_{SMPS} * \frac{V_{SMPS}}{n * V_{DD}}$$

Merging the two equations gives:

$$I_{DD} = I_2 + I_1 * V_{SMPS}^2/(n * V_{DD} * V_1)$$

In run modes, $I = I_1 + I_2$ as the main regulator is a dropout regulator. Assuming the current inefficiency of this regulator can be neglected:

$$I_{DD} = I * V_{SMPS}^2/(n * V_{DD} * V_1)$$

where *I* is the current consumption without SMPS. This equation demonstrates the advantage of using an SMPS, especially at a high VDD, as well as the advantage of decreasing as much as possible the VSMPS voltage. The current consumption of the MCU for each mode of operation, according to its Datasheet, is presented in Table 13.

| Mode | Regulator | Consumption | Wake up time |
|---|---|---|---|
| Run | MR range 1 | 108µA / MHz | N/A |
| | SMPS range 2 High | 40µA / MHz | |
| | MR range 2 | 93µA / MHz | |
| | SMPS range 2 Low | 39µA / MHz | |
| LPRun | LPR | 129µA / MHz | Range 1: 4µs |

| | | | |
|---|---|---|---|
| | | | Range 2: 64µs |
| Sleep | MR range 1 | 32µA / MHz | 6 cycles |
| | SMPS range 2 High | 11.5µA / MHz | |
| | MR range 2 | 30µA / MHz | |
| | SMPS range 2 Low | 13µA / MHz | |
| LPSleep | LPR | 51µA / MHz | 6 cycles |
| Stop 0 | MR range 1 | TBD | 2.7µs in SRAM<br>6.2µs in Flash |
| | MR range 2 | 127µA | |
| Stop 1 | LPR | 11.2µA without RTC<br>11.8µA with RTC | 6.6µs in SRAM<br>7.8µs in Flash |
| Stop 2 | LPR | 2.57µA without RTC<br>2.86µA with RTC | 6.8µs in SRAM<br>8.2µs in Flash |
| Standby | LPR | 0.48µA without RTC<br>0.78µA with RTC | 15.3µs |
| | OFF | 0.11µA without RTC<br>0.42µA with RTC | |
| Shutdown | OFF | 0.03µA without RTC<br>0.23µA with RTC | 306µs |

Table 13 Consumption per mode

## 2.3 Prototype architecture

Figure 14 below depicts the interconnections of the power electronics prototype. The PV is connected with the PMIC through a power rail that carries the energy harvested by the solar panel to the rest of the system. The battery is also connected with the PMIC through a power rail, to allow for the charging of the battery when surplus energy exists or to supply the system when additional energy is required than what the PV can provide.

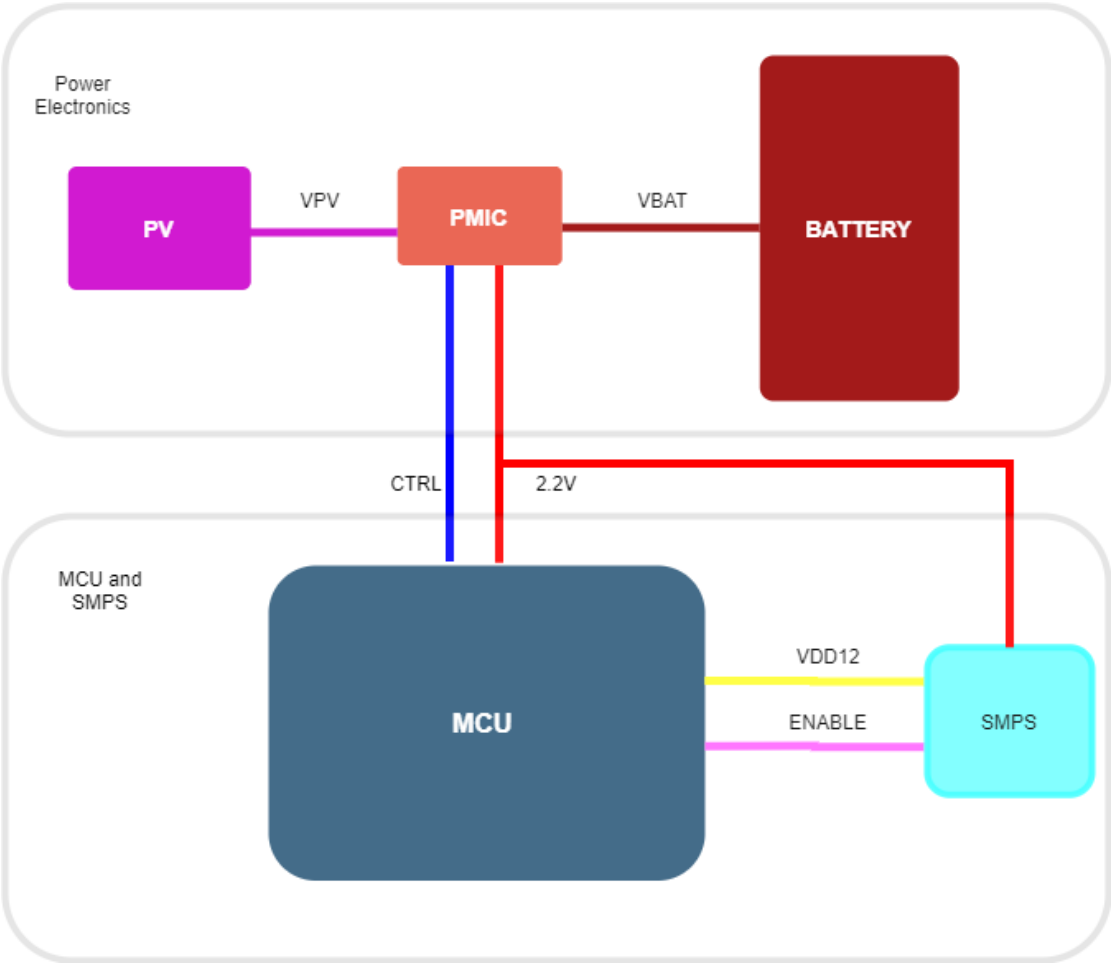


Figure 14 Power electronics interfacing with the MCU

The PMIC is also connected to the MCU through two different lines; a power rail that allows for the powering of the MCU and a control rail that enables the passing of commands between the MCU and the PMIC. Finally, a step down DC-DC converter was used as an external SMPS for the supply of the core of the MCU. This option was included in this prototype since it is also included in the size-unconstrained prototypes of the ASSC and it affects the energy requirements of the system significantly as explained throughout this document.

# 3 Prototype development iterations and PCB manufacturing

For the design, development and evaluation of the power electronics prototype, an iterative process was followed, as detailed in Section 1 of this document. The prototype was used as part of the development of the size-unconstrained prototype in order to optimise the Energy Autonomy Booster. Moreover it was used to update the simulation data of the project, developed as part of **Task T1.4 - Groundwork Energy Simulations** and will be utilised for the development and optimisation of the miniaturised prototype of the project as part of **Task T5.2 - Miniaturized PCB design and prototype development**. This Section details the different iterations of the power electronics prototype. The modifications of the prototype that resulted from the evaluation of each iteration are also described.

## 3.1 Pre-prototyping phase validation

Prior to the integration of the STM32L496 off-the-shelf ST microcontroller in the ASSC, the power consumption of the component had to be evaluated. For this purpose, a commercial development board was used for the initial evaluation of the MCU's energy requirements. The NUCLEO-L496ZG-P STM32 Nucleo-144 [6] reference board is designed around the STM32 microcontrollers in a 144-pin LQFP package. It offers a 32.768 kHz crystal oscillator and an external or internal SMPS to generate Vcore logic supply. The block diagram of the board is depicted in Figure 15 below.

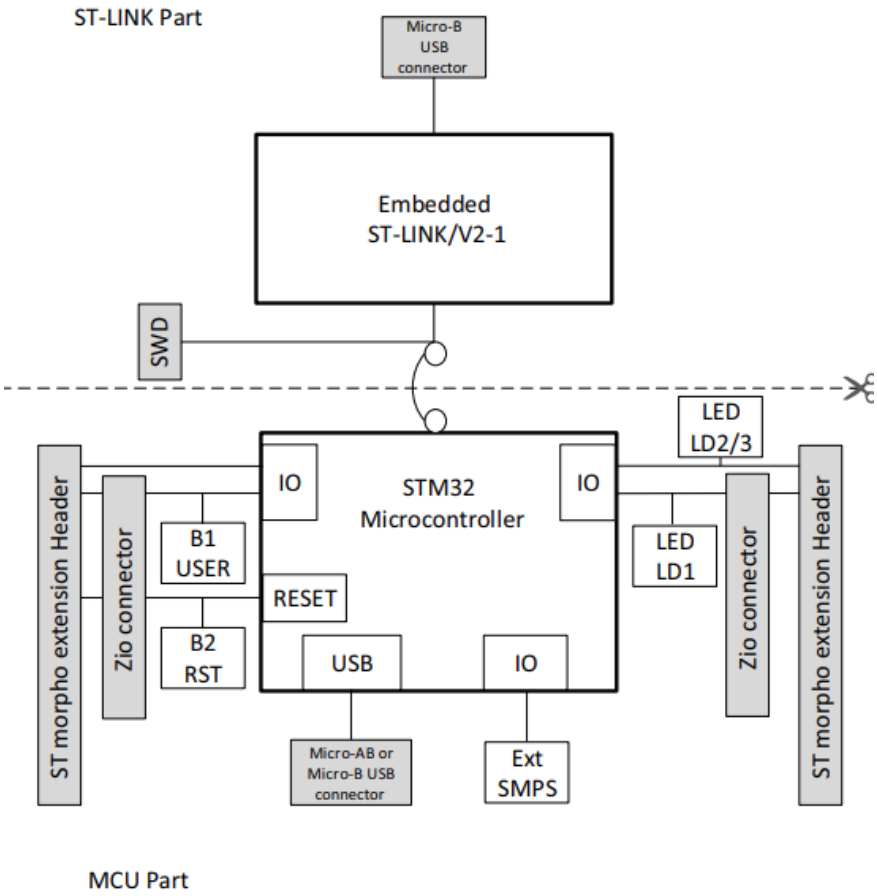


Figure 15 Nucleo-144 block diagram

The operating voltage of the STM32L496 MCU on the development board was 3.3V, no SMPS DC-DC converter was available and the current consumption was measured through a dedicated jumper on the board that allows the measurement of only the supply current of the

microcontroller. In order to define the energy requirements of the device, the current was measured for all the power modes that are supported and for different clock frequencies. In order to evaluate the power characteristics of the MCU individually, no peripherals and sensors were used. Simple code in while (1) was used running from flash memory with the ART accelerator (prefetch) enabled. The results of the measurements are presented in Section 4.1 of this document.

## 3.2 First iteration

In this prototype, the components used were aligned with the ones included in the second iteration of the size-unconstrained prototype. A step down DC-DC converter was used as an external SMPS for the MCU. A control signal was added, in order to be able to turn off the VDD directly through the MCU. Additionally, the 2.2V power rail could be enabled through a hardware button or a jumper in the prototype since the always-on domain was not included. Furthermore, an enable signal was included in the design in order to be able to active and deactive the SMPS for comparison reasons. Appropriate jumpers were also added in the prototype in order to be used as measurement points. The step down converter that was used as an external SMPS for the MCU was chosen from the TPS6220x devices from TI [7]. TPS6220x devices are high-efficiency synchronous step-down converters that operate in a 2.5V to 6V input voltage range and have an adjustable output voltage range from 0.7V to $V_I$. For the prototype, a 1.2V output voltage was used. At light load currents, the converter enters a power save mode with a 15µA typical quiescent current. TPS6220x can provide up to 300mA output current. A typical application schematic of the converter for a fixed output voltage is given in Figure 16 below.

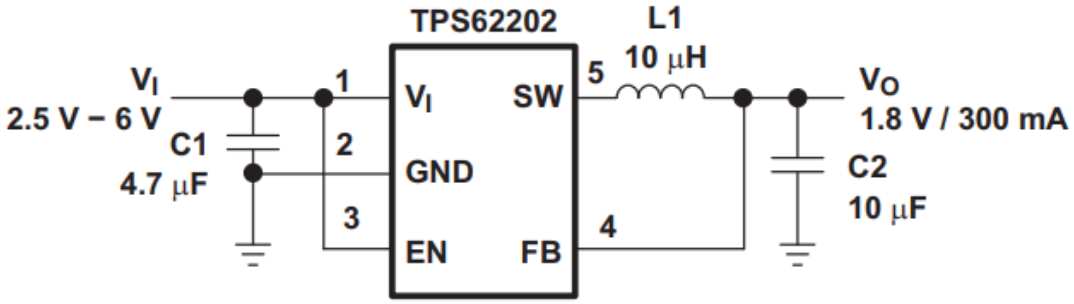


Figure 16 Typical application schematic of TPS6220x [7]

The architecture of the first iteration of the power electronics prototype was presented in Figure 14 above.

## 3.3 Second iteration

The second iteration of the power electronics prototype is based on the third iteration of the size-unconstrained prototype. During the design process of this iteration of the power electronics prototype, special attention has been devoted to the versatility and precision of the measurements. Compared to the first iteration, in this version a number of jumpers were integrated to the design in order to allow for the measurement and supply of different components. Moreover, shunt resistors have been imported to the design and their value was calculated for higher resolution measurements.

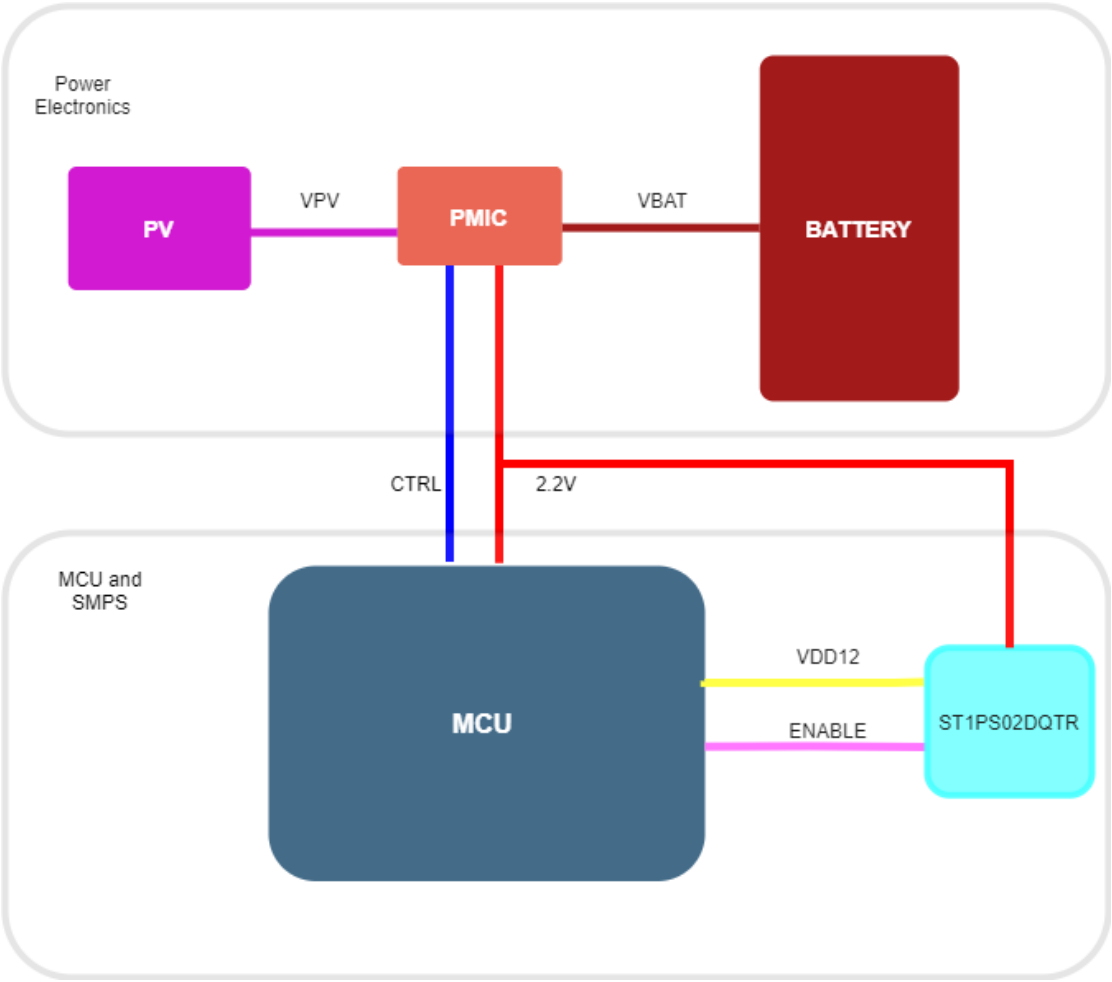


Figure 17 Architecture of the second iteration of the prototype

As depicted in Figure 17, in this iteration TPS6220x was replaced with ST1PS02DQTR [8]. This converter comes in a smaller package, has a smaller quiescent current compared to the previous making it a more suitable solution for the AMANDA system and an adjustable voltage output. A typical application schematic of ST1PS02 for a fixed output voltage is given in Figure 18.

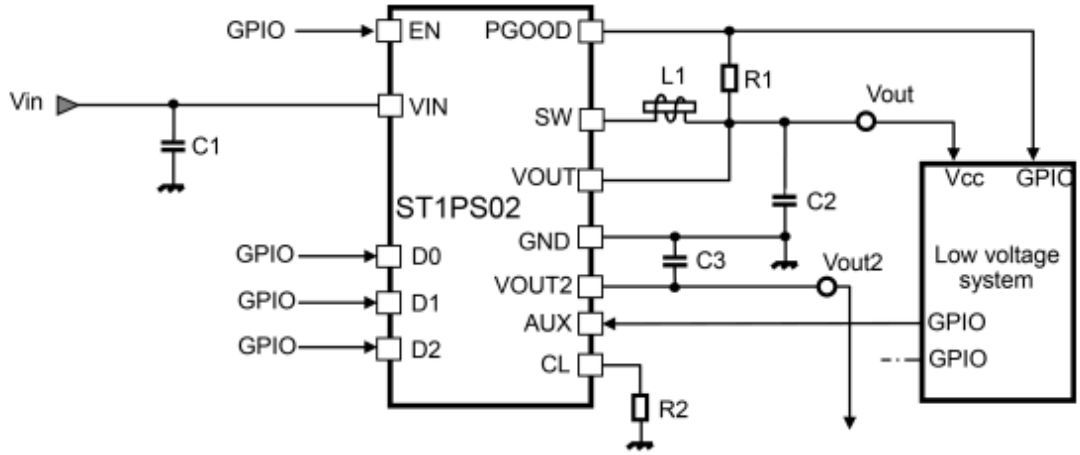


Figure 18 Typical application schematic of ST1PS02DQTR

ST1PS02DQTR has a 500nA input quiescent current at $V_{IN}$ = 3.6V, an 1.8V to 5.5V input operating range, up to 400mA output current and selectable output voltages between 1.0V and 3.3V. Moreover, the output voltage between 1.0V and 1.35V can be selected with a 0.05V step. This feature helps to examine the different VDD12 voltages in order to select the most efficient in terms of energy. The influence of VDD12 voltage to the power efficiency is explained in Section 2.2.1. The evaluation results are presented in Section 4 of this Deliverable.

#### 3.3.1.1 Schematic

In Figure 19, the module selection schematic of the prototype is presented. Several headers has been imported to the design along with shunt resistors to allow the selection or exclusion of the MCU. Furthermore, current measurements can be retrieved from different headers, from JP1 measuring current by placing a multimeter in series with the pin of the header JP1. The power consumption can be subsequently calculated in Watts using Joule's law, according to the following equation:

$$P = V * I$$

Voltage measurements can also be retrieved directly from the jumpers above the shunt resistors using a different form of the above equation:

$$P = V^2 * R$$

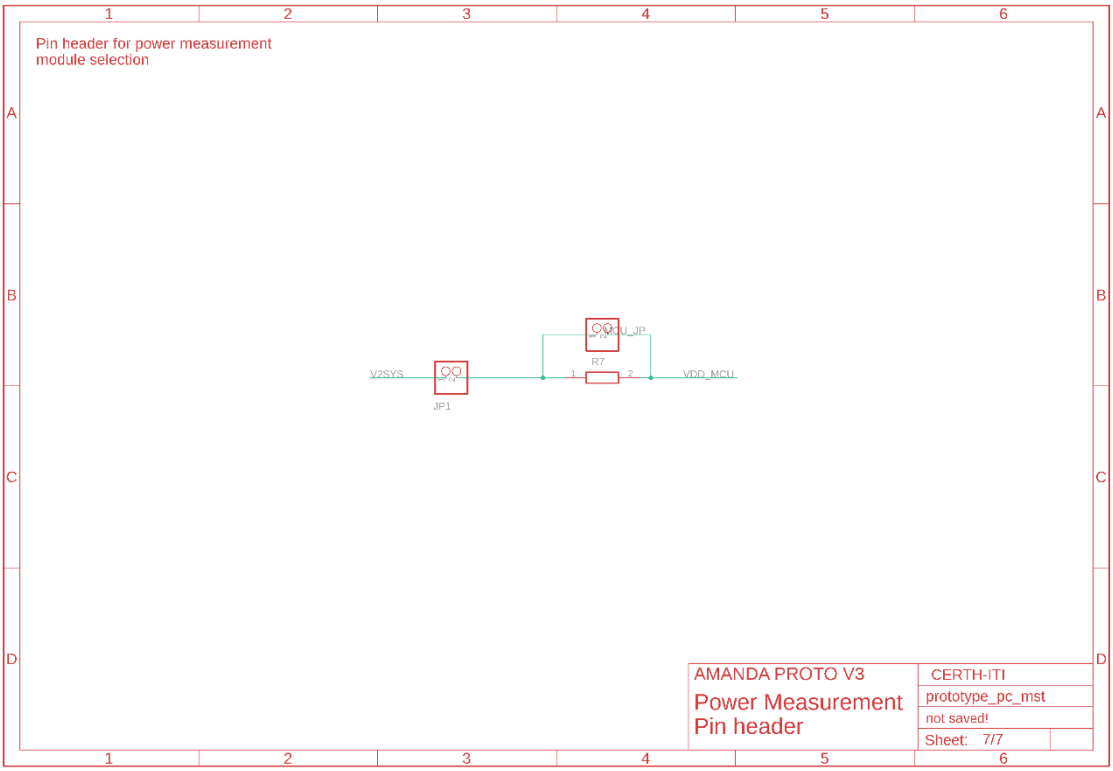


Figure 19 Module selection schematic

#### 3.3.1.2 Layout

Figure 20 illustrates a zoom in an area on the PCB layout of the power electronics prototype, focused on the module selection area. This design has the same dimensions as the layout of the third iteration of the size-unconstrained prototype of the ASSC. For that reason, the design has become finer and the free space has been utilized by importing extensive via stitching. Constant ground vias stitching is performed in order to ensure shorter ground return paths

from the load devices to the power source in the PCB. Thus, it maintains a healthy ground return path obtaining low resistance in the ground plane. That way, the design produces lower heat dissipation since the copper pour is larger and is connected both with the top and bottom layers of the PCB.

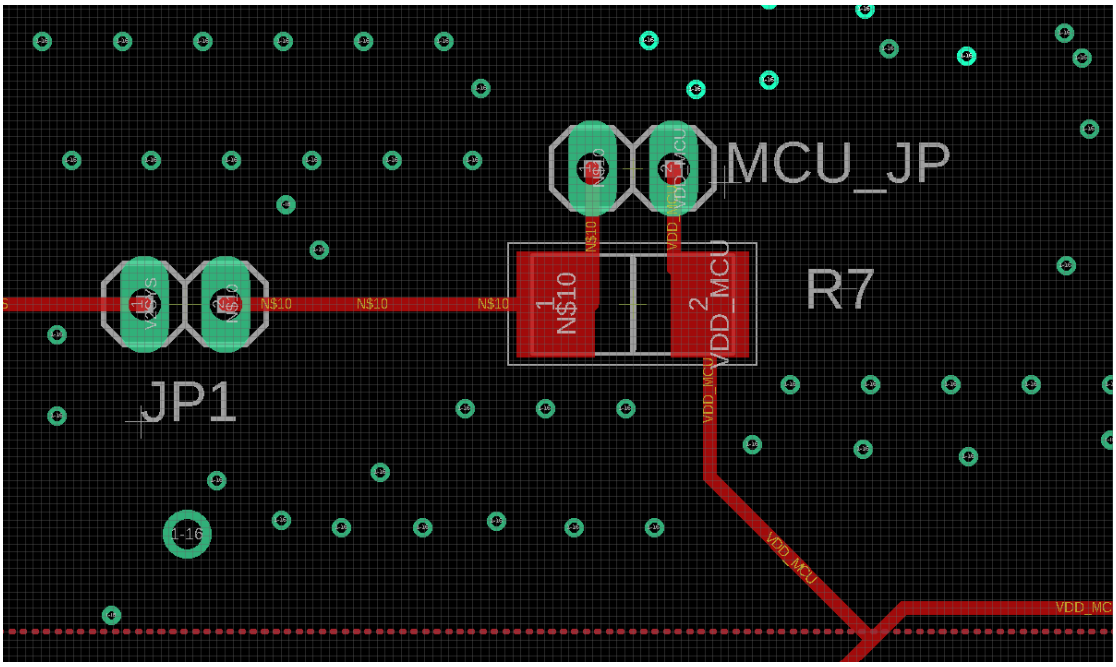


Figure 20 Power electronics prototype layout, module selection area

## 3.4 PCB manufacturing and assembly

The final design of the power electronics prototype is based on the third iteration of the size-unconstrained prototype and consequently the PCB design process is similar. All the recommended manufacturer guidelines were followed so that the designed boards could be manufactured as efficiently as possible while at the same time minimising any errors. In order to achieve an efficient design, all the layouts of the different iterations of the power electronics prototype have been designed following the design rules of the PCB manufacturer. Furthermore, these specifications have been included in the DRC information of the CAD software used, enabling the continuous control of each part of the development process and assuring that way that the PCB design will be manufacturable. The aforementioned settings include information about distances, size, shapes, masks, clearance and layers. All the iterations of the power electronics prototype that are presented in this document are two-layer single-sided boards.

The methodology that has been used for the actual implementation of the prototype boards is the following:

- The creation of the schematic based on the prototype architecture as defined in Section 2 and the third version of the size-unconstrained prototype.
- The design of the layout of the physical device and appropriate verifications
- The fabrication of the designed PCB by an external PCB manufacturer
- The ordering of components according to the BOM of each version
- The PCB assembly (populating the boards with the components)
- The testing and evaluation, both at a PCB level and also in terms of the MCU consumption measurements

The creation of the electrical schematic of the system requires the interpretation of the architectural block diagram into specific circuit arrangement that implements the desired functionality. Having all the required electrical connections and components, the physical layout of the

system is the next step in order to fabricate the actual board. The fabricated PCB should then be assembled. The assembly process requires gathering all the components that populate the bare PCBs and soldering techniques in order to attach them and form a functional device. Finally, hardware-level debugging is performed by utilising laboratory equipment and using the basic firmware routines for validation.

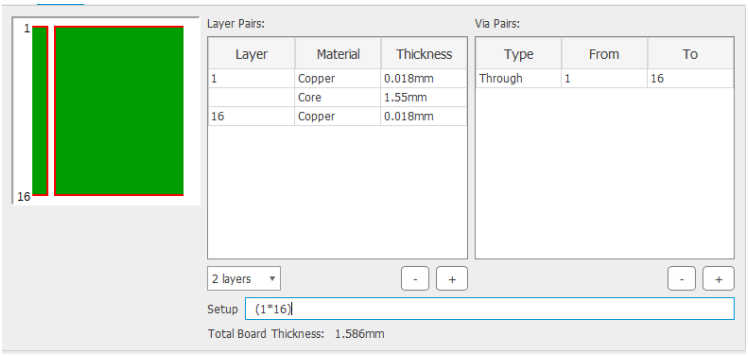


Figure 21 Layers and thickness

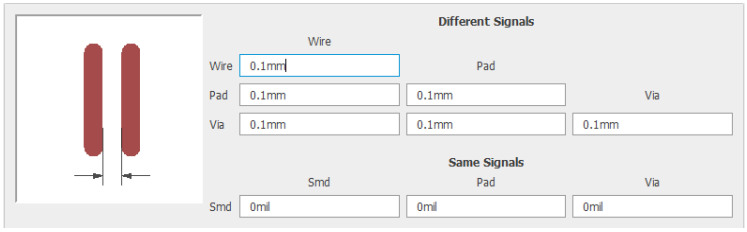


Figure 22 Clearance

Figure 21 shows the two layers of the size-unconstrained prototype of the ASSC from the Eagle PCB design and electrical schematic software while Figure 22 depicts the minimum distance between two traces.

# 4 Prototype evaluation

This Section presents the evaluation of the power electronics prototype in order to determine the efficiency of the system when interfacing with the MCU and to measure the energy availability. The results from the initial evaluation with NUCLEO-L496ZG-P and from the subsequent iterations of the prototype are presented. Finally, a comparison of the evaluation results between the iterations and different set ups is given.

## 4.1 Pre-prototyping evaluation

In this Section, the results of the pre-prototyping phase validation of the MCU, as detailed in Section 3.1 above, are presented.

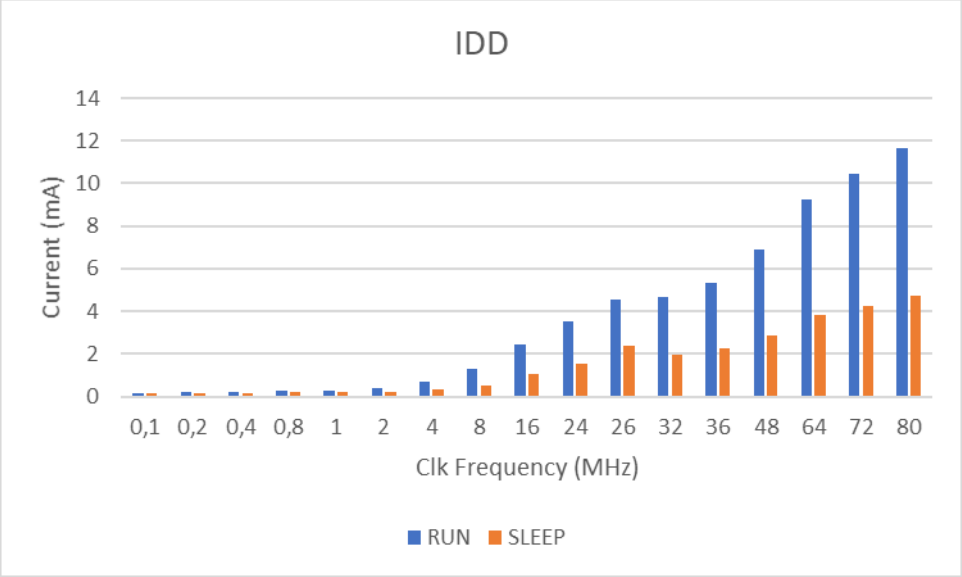


Figure 23 Current consumption in run and sleep mode

Figure 23 illustrates the supply current for both run and sleep mode. The current was measured for the frequency range from 100kHz up to 80MHz, the maximum frequency that the STM32L496 MCU supports. As a clock source, the MSI was used for a frequency range between 0.1 - 48MHz while the PLL was utilised for higher frequencies. As depicted in Figure 24, the current was also measured for the low-power run mode that the MCU supports which is available only for clock frequencies of up to 2MHz.

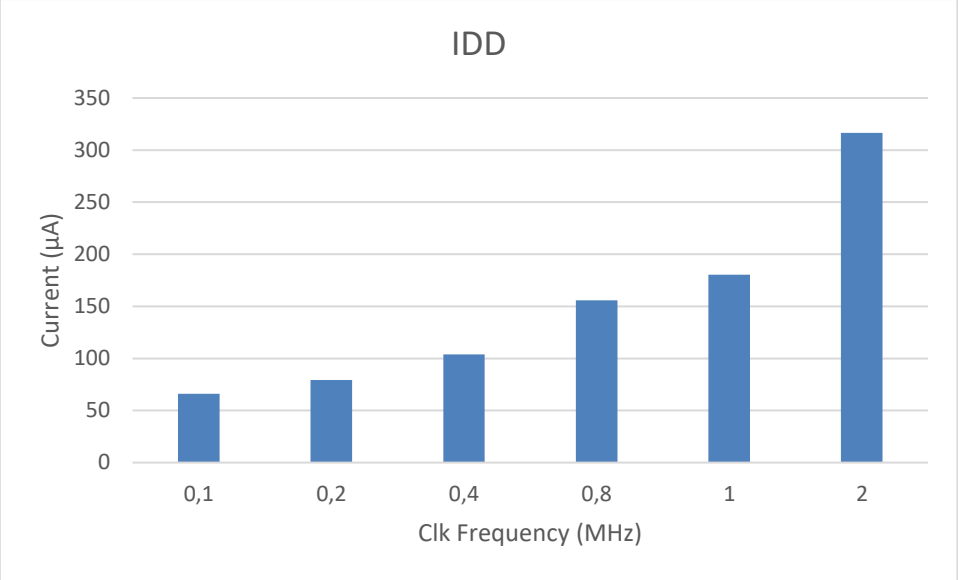


Figure 24 Current consumption in LPRun mode

The energy consumption for the other power modes that the MCU supports was also measured. The standby, shutdown and the three stop modes were also evaluated. As mentioned in **Deliverable D1.12 - Architecture design of the AMANDA system v3**, an important characteristic of the system is that the MCU, together with most of the ASSC's components can be completely shut down when not required with only the always-on domain staying active. Powering down the MCU minimises the energy requirements of the system since it eliminates all the leakages and the standby currents that cumulatively affect the energy consumption of the ASSC. Nevertheless, these modes were examined, in order to further minimise the consumption of the ASSC when it is running by utilizing them between the measurements and the processing with interrupt-based implementations. Figure 25 presents the power consumption of the MCU according to the measured current in each mode for a supply voltage of 3.3V. A summary of the power consumption for the standby, shutdown, stop 0, stop 1 and stop 2 power modes is given in Table 14 below.

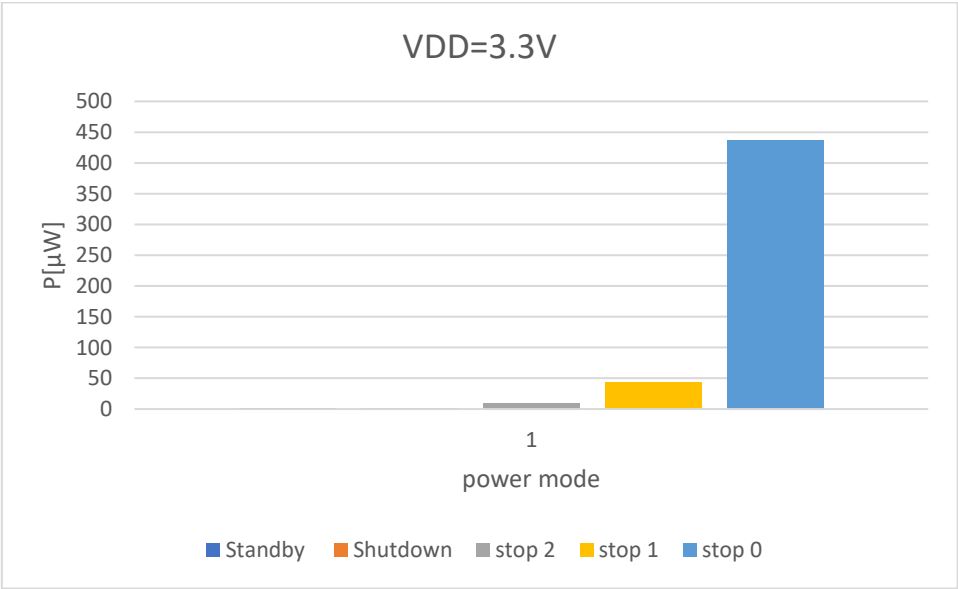


Figure 25 Power consumption in different modes

| Mode | Consumption |
|---|---|
| Standby | 0.1μA |
| Shutdown | 0.08μA |
| Stop 0 | 134.2μA |
| Stop 1 | 13.3μA |
| Stop 2 | 2.9μA |

Table 14 Power consumption in different modes summary

As mentioned in the previous Section, apart from the standby, shutdown and Stop 0, 1, 2 power modes, the MCU also has the ability to be supplied by an external DC-DC converter that can be used as an external SMPS. That way, the integrated main regulator of the microcontroller can be substituted thus the energy consumption can be further reduced in run, sleep and stop 1 modes. This option was adopted for the AMANDA ASSC, as detailed in **Deliverable D5.1 - 1st Unconstrained Prototype.** In order to be able to support the rest of the power modes, the SMPS will be enabled and disabled by the MCU of the ASSC if a power mode that requires the disconnection of the SMPS needs to be entered. In the next Section, an evaluation of the power consumption of the system is performed both with and without an external SMPS on the prototype.

## 4.2 First iteration evaluation

The results of the energy evaluation of the first iteration of the power electronics prototype are presented in this Section. For the evaluation process, the supply current of the MCU was measured for different clock frequencies and operation modes. The measurements where conducted on the MCU while it was supplied by the energy provided from the power management block. As mentioned in Section 3.2 above, TSP6220 was used as an SMPS for the MCU in this iteration of the prototype. Figure 26 presents the supply current of the MCU in run mode in the entire frequency range of the system clock. The blue measurements were conducted with the SMPS disabled and the red ones with the SMPS enabled. Figure 27 depicts the same measurements for the sleep mode.

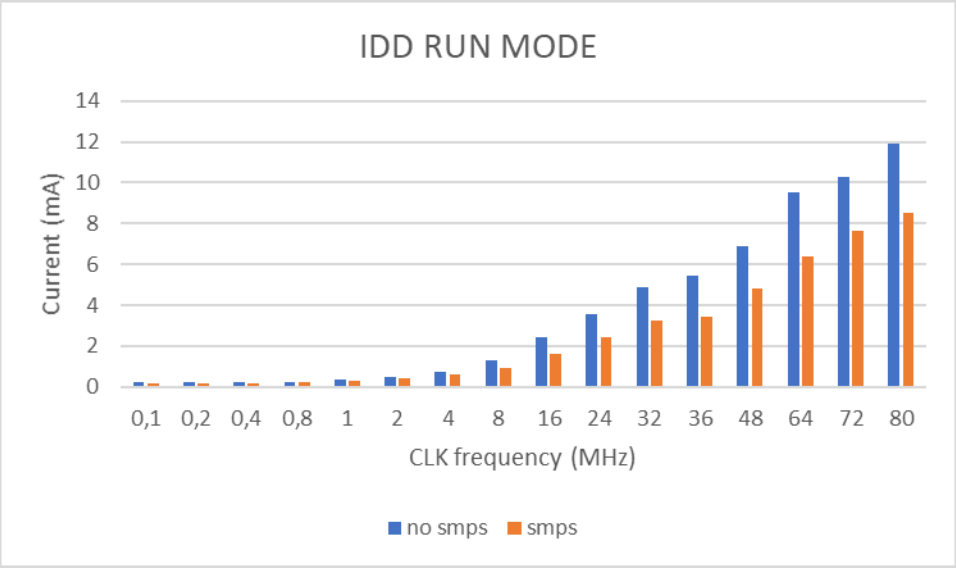


Figure 26 Supply current in run mode with and without SMPS

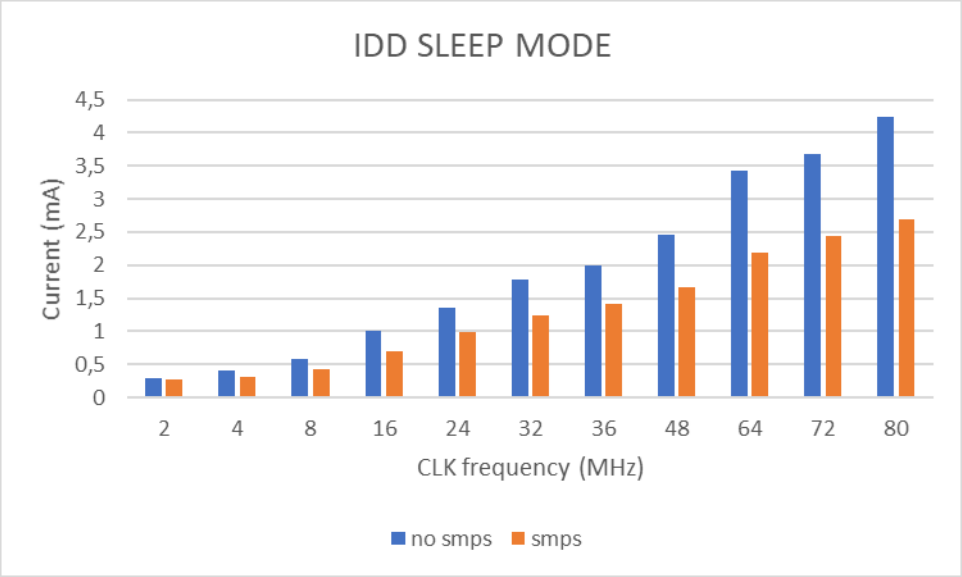


Figure 27 Supply current in sleep mode with and without SMPS

It is obvious from the Figures that the use of the SMPS optimises the power efficiency of the MCU, both in run and sleep mode. From the measurements, it was also observed that the improvement of consumption was not optimised as expected according to [4] and [9]. The main reason for this is the voltage scaling that the MCU supports and the output voltage of the DC-DC converter that was used in the prototype. Moreover, as mentioned in Section 2.2.1, the voltage provided by the external converter should be at least 50mV higher than the internally produced voltage in order to deactivate the main regulator. The internally produced voltages of the core of the microcontroller are 1V for the frequency range 2 and 1.2V for the frequency range 1 as mentioned in [5]. This means that the SMPS voltage should be:

- At least 1.05V, for a frequency below 26MHz
- At least 1.25V, for higher frequencies

These voltages take into account the fact that the SMPS voltage should be as low as possible, according to the equations presented in Section 2.2.1. The best efficiency in each range could be achieved with different voltages. This is the reason why the reduction of the current was not as expected in the entire frequency range. In order to overcome this issue, the converter was replaced in the next iteration of the prototype, as mentioned in Section 3.3.

## 4.3 Second iteration evaluation

The same methodology was conducted for the second iteration of the prototype. The results presented here are only with the SMPS enabled since the consumption without it was evaluated in the previous versions and it is not suitable for the AMANDA, and it will be only disabled in case one of the two stop modes that don't support the option of SMPS need to be used.
As discussed in Section 3.3 above, the step down converter that was included in this iteration has a selectable output voltage. According to [5], the SMPS voltage should not exceed the 1.32V in any case, while additionally, it should be at least 1.2V if it needs to be used for the entire frequency range. This is the reason behind the testing of the two different output voltages. As depicted in Figure 28 and Figure 29 the current was measured for 1.2V and 1.25V outputs.

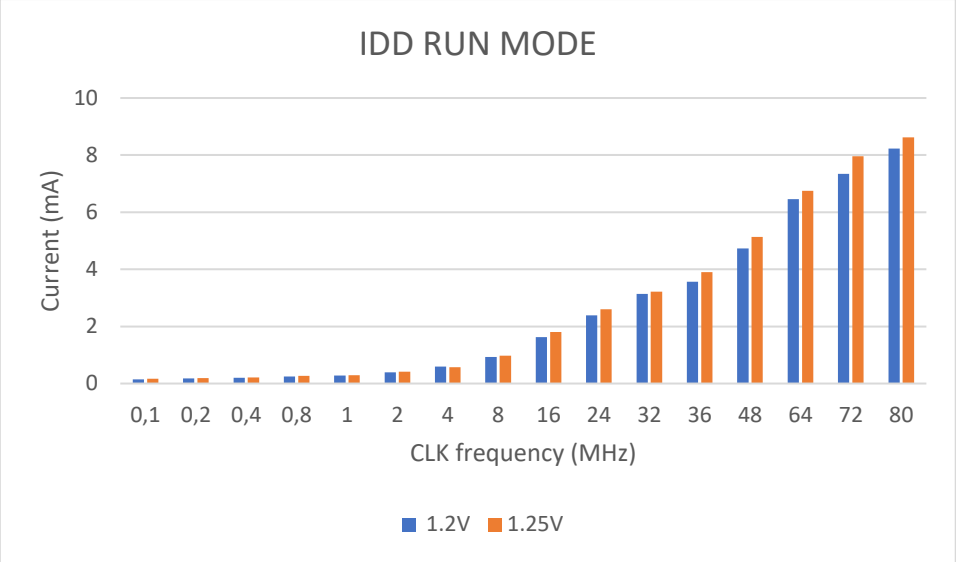


Figure 28 Supply current for different SMPS voltages in run mode

The measured voltages on the output of ST1PS02DQTR were 1.21V and 1.266V respectively. As it can be seen from the Figures, the current consumption was lower when a lower voltage was used on the converter.

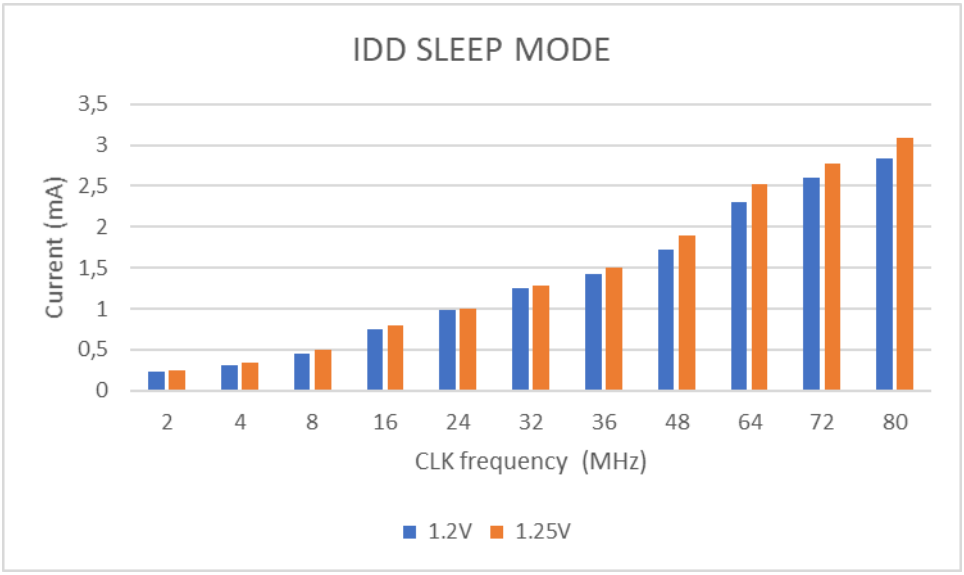


Figure 29 Supply current for different SMPS voltages in sleep mode

## 4.4 Comparison results

A comparison of the current consumption between the iterations is presented in Figure 30. The diagram represents the consumption from the first iteration of the prototype with the SMPS disabled and enabled as well as the consumption from the second prototype for 1.2V and 1.25V respectively. From the comparison results, it is obvious that using the SMPS option for the MCU of the AMANDA ASSC helps to reduce the power consumption and thus it allows the extension of the time that the system can be turned on. Moreover, the consumption is further reduced as the SMPS voltage is reduced. The difference in the consumption with the 1.25V is better observed in higher frequencies due to the voltage-scaling feature that the microcontroller includes. The consumption of the first iteration and the second one with the 1.2V are close enough with the second one being slightly improved. The current consumption

that is presented in these diagrams apart from the voltage of the converter is also affected by the consumption of the converter itself, which, as mentioned in Section 3.3, is lower in the second iteration of the prototype.

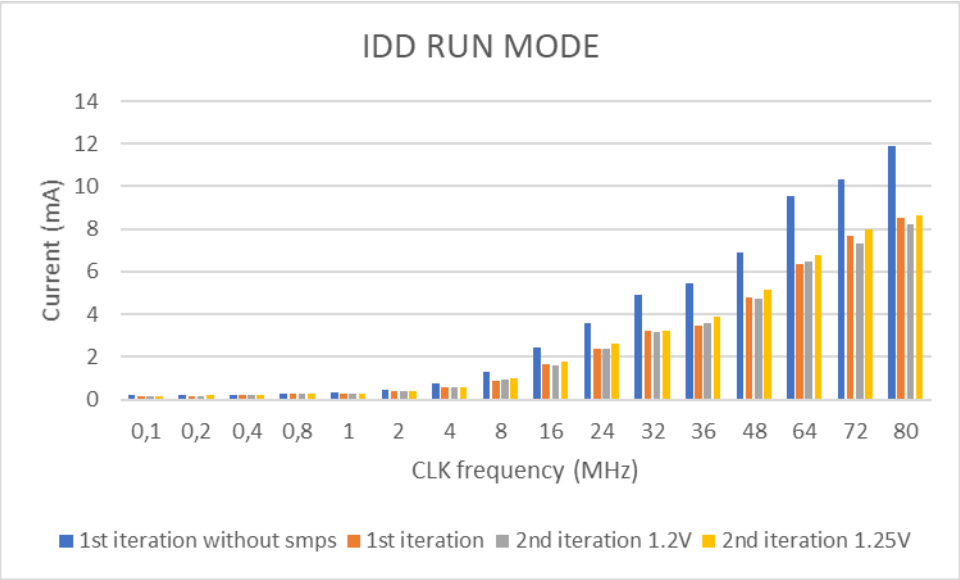


Figure 30 Comparison of current consumption

# 5 Conclusions and future work

**Deliverable D3.6 - Power generation boards with appropriate measurement points and chosen MCU** presents the design and development of a power electronics prototype to evaluate the Energy Management block of the AMANDA that involves the power electronics of the ASSC as well as the interfacing of the electronics with the system's MCU. D3.6 signifies the completion of **Task T3.4 - Power electronics interfacing with the main system microcontroller.** The focus of Task T3.4 was on the integration of the energy-providing components, the hardware management for that energy and the storage element.

This Deliverable was used as an input for the development of the size-unconstrained prototype of **T5.1 - First size unconstrained design and prototype**. It will also be used for the development of the miniaturised prototype, as an input for **Deliverable D5.2 - Miniaturized PCB Prototype**. Moreover, it will be utilised for the evaluation of both the individual components and the final, integrated system, as part of **Deliverables D6.2 - Characterisation/test reports of individual components in lab environment** and **D6.3 - Characterisation/test reports of integrated AMANDA platform in lab environment** respectively.

# Bibliography

[1] M. Singh, Power Electronics, Mc Graw Hill, 2006.

[2] P. Krein, Elements of Power Electronics, Oxford University Press, 2014.

[3] E-peas semiconductors, “Highly-efficient, regulated dual-output, ambient energy,” 2018.

[4] STMicroelectronics, “STM32L496xx-Ultra-low-power Arm® Cortex®-M4 32-bit MCU+FPU, 100 DMIPS, Datasheet,” 2021. [Online].

[5] STMicroelectronics, “RM0351- STM32L47xxx, STM32L48xxx, STM32L49xxx and STM32L4Axxx, Reference Manual,” 2021. [Online].

[6] STMicroelectronics, “STM32 Nucleo-144 boards,” 2021.

[7] T. Instruments, “TPS6220x-High Efficiency , SOT23 Step-Down, DC-DC Converter,” 2015. [Online].

[8] STMicroelectronics, “ST1PS02-400 mA nano-quiescent synchronous step-down converter with digital voltage-Datasheet,” 2020. [Online].

[9] STMicroelectronics, “AN4978-Design recommendations for STM32L4xxx with external SMPS, for ultra-low-power applications with high performance-Application note,” 2018. [Online].

# 6 Appendix - Bill of Materials

The Appendix of this Document lists the BoM for the final iteration of the power electronics prototype.

| Part | Value | Device | Package | Description |
|---|---|---|---|---|
| AOUT | | TESTPOINTROUND1MM | TESTPOINT_ROUND_1MM | Test Point |
| B0/BMISO | | TESTPOINTROUND1MM | TESTPOINT_ROUND_1MM | Test Point |
| B6/LR_RST | | TESTPOINTROUND1MM | TESTPOINT_ROUND_1MM | Test Point |
| B7/BSCL | | TESTPOINTROUND1MM | TESTPOINT_ROUND_1MM | Test Point |
| B8/BSDA | | TESTPOINTROUND1MM | TESTPOINT_ROUND_1MM | Test Point |
| B9/BSCK | | TESTPOINTROUND1MM | TESTPOINT_ROUND_1MM | Test Point |
| B10/LOR_CS | | TESTPOINTROUND1MM | TESTPOINT_ROUND_1MM | Test Point |
| B11/ANT_SW | | TESTPOINTROUND1MM | TESTPOINT_ROUND_1MM | Test Point |
| B12/BMOSI | | TESTPOINTROUND1MM | TESTPOINT_ROUND_1MM | Test Point |
| BATT | PINHD-1X2 | 1X02 | PIN HEADER | PINHD-1X2 |
| BATT_LED | | PINHD-1X2 | 1X02 | PIN HEADER |
| C3 | 10u | C-EUC0805 | C0805 | CAPACITOR, European symbol |
| C4 | 10u | C-EUC1608 | C1608 | CAPACITOR, European symbol |
| C5 | 10u | C-EUC1608 | C1608 | CAPACITOR, European symbol |
| C10 | 220n | C-EUC0603 | C0603 | CAPACITOR, European symbol |
| C20 | 10u | C-EUC0805 | C0805 | CAPACITOR, European symbol |
| C21 | 10u | C-EUC0805 | C0805 | CAPACITOR, European symbol |
| C22 | 22u | C-EUC0805 | C0805 | CAPACITOR, European symbol |
| C23 | 10u | C-EUC0805 | C0805 | CAPACITOR, European symbol |
| C25 | 10u | C-EUC0805 | C0805 | CAPACITOR, European symbol |
| C26 | 10u | C-EUC0805 | C0805 | CAPACITOR, European symbol |
| CBAT | | CPOL-EUCT3528 | CT3528 | POLARIZED CAPACITOR, European symbol |

| | | | | |
|---|---|---|---|---|
| CM1 | 100n | C-EUC0402 | C0402 | CAPACITOR, European symbol |
| CM2 | 4.7u | C-EUC0402 | C0402 | CAPACITOR, European symbol |
| CM3 | 100n | C-EUC0402 | C0402 | CAPACITOR, European symbol |
| CM4 | 4.7u | C-EUC0402 | C0402 | CAPACITOR, European symbol |
| CM5 | 100n | C-EUC0402 | C0402 | CAPACITOR, European symbol |
| CM6 | 4.7u | C-EUC0402 | C0402 | CAPACITOR, European symbol |
| CM7 | 100n | C-EUC0402 | C0402 | CAPACITOR, European symbol |
| CM8 | 4.7u | C-EUC0402 | C0402 | CAPACITOR, European symbol |
| CM9 | 100n | C-EUC0402 | C0402 | CAPACITOR, European symbol |
| CM10 | 4.7u | C-EUC0402 | C0402 | CAPACITOR, European symbol |
| CM11 | 100n | C-EUC0402 | C0402 | CAPACITOR, European symbol |
| CM12 | 4.7u | C-EUC0402 | C0402 | CAPACITOR, European symbol |
| CM13 | 100n | C-EUC0402 | C0402 | CAPACITOR, European symbol |
| CM14 | 4.7u | C-EUC0402 | C0402 | CAPACITOR, European symbol |
| CM15 | 100n | C-EUC0402 | C0402 | CAPACITOR, European symbol |
| CM16 | 4.7u | C-EUC0402 | C0402 | CAPACITOR, European symbol |
| CM17 | 100n | C-EUC0402 | C0402 | CAPACITOR, European symbol |
| CM18 | 4.7u | C-EUC0402 | C0402 | CAPACITOR, European symbol |
| EXT_CLK | | TESTPOINTROUND1MM | TESTPOINT_ROUND_1MM | Test Point |
| IC1 | ST1PS02DQTR | ST1PS02DQTR | QFN40P170X200X55-12N | Switching Voltage Regulators 400mA Nano-Quiescent Synchronous step-down converter digital volt Power Good AUX |
| | | | | |
| JP1 | | PINHD-1X2 | 1X02 | PIN HEADER |
| JP2 | | PINHD-2X4 | 2X04 | PIN HEADER |
| L11 | LPS4012-103MRB | LPS4012-103MRB | IND_LPS4012-103MRB | Power inductor, shielded, 20/30% tol, |

| | | | | |
|---|---|---|---|---|
| | | | | SMT, RoHS, lead-free, halogen-free |
| L20 | LPS4012-103MRB | LPS4012-103MRB | IND_LPS4012-103MRB | Power inductor, shielded, 20/30% tol, SMT, RoHS, lead-free, halogen-free |
| L21 | LPS4012-103MRB | LPS4012-103MRB | IND_LPS4012-103MRB | Power inductor, shielded, 20/30% tol, SMT, RoHS, lead-free, halogen-free |
| LBAT | | LEDCHIPLED_0603 | CHIPLED_0603 | LED |
| LBOO | | LEDCHIPLED_0603 | CHIPLED_0603 | LED |
| LBUC | | LEDCHIPLED_0603 | CHIPLED_0603 | LED |
| LD | RGBLED_CALUMIX-SML-LX0404 | RGBLED_CALU-MIX-SML-LX0404 | LUMIX-SML-LX0404 | RGB LED, common-anode |
| LD3P | TPS780DDC | TPS780DDC | SOT23-5L | |
| LDO_USB | TPS780DDC | TPS780DDC | SOT23-5L | |
| LED_PWR | | PINHD-1X3 | 1X03 | PIN HEADER |
| LGND | | PINHD-1X2 | 1X02 | PIN HEADER |
| LSRC | | LEDCHIPLED_0603 | CHIPLED_0603 | LED |
| LUSB | | LEDCHIPLED_0603 | CHIPLED_0603 | LED |
| LV3SYS | | LEDCHIPLED_0603 | CHIPLED_0603 | LED |
| LVHV | | LEDCHIPLED_0603 | CHIPLED_0603 | LED |
| MCU_JP | | PINHD-1X2 | 1X02 | PIN HEADER |
| MCU_SW | | MA05-1 | MA05-1 | PIN HEADER |
| NRST | | TESTPOINTROUND1MM | TESTPOINT_ROUND_1MM | Test Point |
| PA0/BAT_MEAS | | TESTPOINTROUND1MM | TESTPOINT_ROUND_1MM | Test Point |
| PA1/R_LED | | TESTPOINTROUND1MM | TESTPOINT_ROUND_1MM | Test Point |
| PA2/G_LED | | TESTPOINTROUND1MM | TESTPOINT_ROUND_1MM | Test Point |
| PA3/MCU_LATCH | | TESTPOINTROUND1MM | TESTPOINT_ROUND_1MM | Test Point |
| PA4/CI_HS | | TESTPOINTROUND1MM | TESTPOINT_ROUND_1MM | Test Point |
| PA7/B_LED | | TESTPOINTROUND1MM | TESTPOINT_ROUND_1MM | Test Point |
| PA9/STAT1 | | TESTPOINTROUND1MM | TESTPOINT_ROUND_1MM | Test Point |
| PA10/STAT2 | | TESTPOINTROUND1MM | TESTPOINT_ROUND_1MM | Test Point |
| PA11/BLE_CS | | TESTPOINTROUND1MM | TESTPOINT_ROUND_1MM | Test Point |

| | | | | |
|---|---|---|---|---|
| PA12/NFC_FD | | TESTPOINTROUND1MM | TESTPOINT_ROUND_1MM | Test Point |
| PA13/SWDIO | | TESTPOINTROUND1MM | TESTPOINT_ROUND_1MM | Test Point |
| PB0 | | TESTPOINTROUND1MM | TESTPOINT_ROUND_1MM | Test Point |
| PB2/FR_CS | | TESTPOINTROUND1MM | TESTPOINT_ROUND_1MM | Test Point |
| PB10/MUTX | | TESTPOINTROUND1MM | TESTPOINT_ROUND_1MM | Test Point |
| PB12/LSF_EN | | TESTPOINTROUND1MM | TESTPOINT_ROUND_1MM | Test Point |
| PB13/SCK | | TESTPOINTROUND1MM | TESTPOINT_ROUND_1MM | Test Point |
| PB15/V33EN | | TESTPOINTROUND1MM | TESTPOINT_ROUND_1MM | Test Point |
| PC0/SCL | | TESTPOINTROUND1MM | TESTPOINT_ROUND_1MM | Test Point |
| PC1/SDA | | TESTPOINTROUND1MM | TESTPOINT_ROUND_1MM | Test Point |
| PC2/MISO | | TESTPOINTROUND1MM | TESTPOINT_ROUND_1MM | Test Point |
| PC3/MOSI | | TESTPOINTROUND1MM | TESTPOINT_ROUND_1MM | Test Point |
| PC4/BAT_EN | | TESTPOINTROUND1MM | TESTPOINT_ROUND_1MM | Test Point |
| PC13 | | TESTPOINTROUND1MM | TESTPOINT_ROUND_1MM | Test Point |
| PC14 | | TESTPOINTROUND1MM | TESTPOINT_ROUND_1MM | Test Point |
| PC15 | | TESTPOINTROUND1MM | TESTPOINT_ROUND_1MM | Test Point |
| PD9/MURX | | TESTPOINTROUND1MM | TESTPOINT_ROUND_1MM | Test Point |
| PH0 | | TESTPOINTROUND1MM | TESTPOINT_ROUND_1MM | Test Point |
| PH1 | | TESTPOINTROUND1MM | TESTPOINT_ROUND_1MM | Test Point |
| PMIC | AEM10941 | AEM10941 | QFN50P500X500X90-29N | AEM10941 Highly Efficient, Dual Regulated Output, Ambient Energy Manager for up to 7 cells solar panels with optional primary battery |
| PRIM_SEL | | PINHD-1X2 | 1X02 | PIN HEADER |
| PV | PINHD-1X2 | 1X02 | PIN HEADER | PINHD-1X2 |
| R1 | CRM1206AFX-1R00ELF | CRM1206AFX-1R00ELF | RESC3116X65N | BOURNS - CRM1206AFX-1R00ELF - RES, AEC-Q200, THICK FILM, 1R, 1%, 1206 |

| | | | | |
|---|---|---|---|---|
| R2 | RCWE0805R500FKEA | RCWE0805R500FKEA | RESC2013X65N | Thick Film Surface Mount Chip Resistors Wraparound, Extremely Low Value |
| R3 | 1k | R-EU_R0805 | R0805 | RESISTOR, European symbol |
| R4 | 0 | R-EU_R0603 | R0603 | RESISTOR, European symbol |
| R5 | 1M | R-EU_R0603 | R0603 | RESISTOR, European symbol |
| R6 | CRM0805-FX-1000ELF | CRM0805-FX-1000ELF | RESC2012X60N | Current Sense Resistors - SMD 100 OHM 1% 1/4W 100PPM |
| R7 | CRM2512-JW-330ELF | CRM2512-JW-330ELF | RESC6331X80N | Current Sense Resistors - SMD 2watts 5% 33ohms 200 PPM 2512 |
| R8 | 200K | R-EU_R0805 | R0805 | RESISTOR, European symbol |
| R9 | 300K | R-EU_R0805 | R0805 | RESISTOR, European symbol |
| R10 | 10k | R-EU_R0805 | R0805 | RESISTOR, European symbol |
| R11 | 100k | R-EU_R0805 | R0805 | RESISTOR, European symbol |
| R12 | 82k | R-EU_R0805 | R0805 | RESISTOR, European symbol |
| R20 | 10k | R-EU_R0805 | R0805 | RESISTOR, European symbol |
| R27 | 100k | R-EU_R0805 | R0805 | RESISTOR, European symbol |
| R28 | 100k | R-EU_R0805 | R0805 | RESISTOR, European symbol |
| R29 | 2.2 | R-EU_R0805 | R0805 | RESISTOR, European symbol |
| RF1 | 18M | R-EU_R0805 | R0805 | RESISTOR, European symbol |
| RF2 | 15M | R-EU_R0805 | R0805 | RESISTOR, European symbol |
| RL1 | 270 | R-EU_R0805 | R0805 | RESISTOR, European symbol |
| RL2 | 100 | R-EU_R0805 | R0805 | RESISTOR, European symbol |
| RL3 | 120 | R-EU_R0805 | R0805 | RESISTOR, European symbol |
| RL4 | 100 | R-EU_R0805 | R0805 | RESISTOR, European symbol |
| RL20 | 100 | R-EU_R0805 | R0805 | RESISTOR, European symbol |
| RL21 | 100 | R-EU_R0805 | R0805 | RESISTOR, European symbol |

| | | | | |
|---|---|---|---|---|
| RL23 | 100 | R-EU_R0805 | R0805 | RESISTOR, European symbol |
| RL24 | 100 | R-EU_R0805 | R0805 | RESISTOR, European symbol |
| RL25 | 100 | R-EU_R0805 | R0805 | RESISTOR, European symbol |
| RL26 | 100 | R-EU_R0805 | R0805 | RESISTOR, European symbol |
| RL27 | 100 | R-EU_R0402 | R0402 | RESISTOR, European symbol |
| RL28 | 100 | R-EU_R0402 | R0402 | RESISTOR, European symbol |
| RL29 | 100 | R-EU_R0402 | R0402 | RESISTOR, European symbol |
| RL30 | 100 | R-EU_R0402 | R0402 | RESISTOR, European symbol |
| RL31 | 100 | R-EU_R0402 | R0402 | RESISTOR, European symbol |
| RS1 | 39M | R-EU_R0805 | R0805 | RESISTOR, European symbol |
| RS2 | 286k | R-EU_R0805 | R0805 | RESISTOR, European symbol |
| RS3 | 1.607M | R-EU_R0805 | R0805 | RESISTOR, European symbol |
| RS4 | 13.1M | R-EU_R0805 | R0805 | RESISTOR, European symbol |
| RST | | 10-XX | B3F-10XX | OMRON SWITCH |
| SEL0 | | SOLDER-JUMPER_2WAYT | SJ_2 | Solder Jumper |
| SEL1 | | SOLDER-JUMPER_2WAYT | SJ_2 | Solder Jumper |
| SEL4 | | SOLDER-JUMPER_2WAYT | SJ_2 | Solder Jumper |
| SEL5 | | SOLDER-JUMPER_2WAYT | SJ_2 | Solder Jumper |
| SEL6 | | SOLDER-JUMPER_2WAYT | SJ_2 | Solder Jumper |
| T14 | NX3008NBKMB | NX3008NBKMB | SOT883(B) | 30 V, single N-channel Trench MOSFET |
| T15 | NX3008PBKMB | NX3008PBKMB | SOT883(B) | 30 V, single P-channel Trench MOSFET |
| T26 | NX3008NBKMB | NX3008NBKMB | SOT883(B) | 30 V, single N-channel Trench MOSFET |
| T27 | NX3008PBKMB | NX3008PBKMB | SOT883(B) | 30 V, single P-channel Trench MOSFET |
| TL1 | NX3008NBKMB | NX3008NBKMB | SOT883(B) | 30 V, single N-channel Trench MOSFET |
| TL2 | NX3008NBKMB | NX3008NBKMB | SOT883(B) | 30 V, single N-channel Trench MOSFET |

| | | | | |
|---|---|---|---|---|
| TL3 | NX3008NBKMB | NX3008NBKMB | SOT883(B) | 30 V, single N-channel Trench MOSFET |
| TL4 | NX3008NBKMB | NX3008NBKMB | SOT883(B) | 30 V, single N-channel Trench MOSFET |
| TL5 | NX3008NBKMB | NX3008NBKMB | SOT883(B) | 30 V, single N-channel Trench MOSFET |
| TP1 | | TESTPOINTROUND1MM | TESTPOINT_ROUND_1MM | Test Point |
| TP5 | | TESTPOINTROUND1MM | TESTPOINT_ROUND_1MM | Test Point |
| U2 | LSF0204 | LSF0204 | TSSOP_14 | Level Shifter |
| U3 | STM32L496V-LQFP100GT6 | STM32L496V-LQFP100GT6 | LQFP100_14X14 | STM32L496VX LQFP100 |
| USB | 1050170001 | 1050170001 | MOLEX_1050170001 | USB connector |
| USB_CHR | | PINHD-1X3 | 1X03 | PIN HEADER |
| V2EN | | PINHD-1X2 | 1X02 | PIN HEADER |
| V2EN_BT | | 10-XX | B3F-10XX | OMRON SWITCH |
| V2SYS_PWR | | PINHD-1X2 | 1X02 | PIN HEADER |
| VDD12 | | TESTPOINTROUND1MM | TESTPOINT_ROUND_1MM | Test Point |
| VDDUSB | | TESTPOINTROUND1MM | TESTPOINT_ROUND_1MM | Test Point |
| VDD_MCU | | TESTPOINTROUND1MM | TESTPOINT_ROUND_1MM | Test Point |